

Electronic Supplementary Information for:

**Side-chain effects on the co-existence of emergent
nanopatterns in amino acid adlayers on graphene**

Joel B. Awuah^a and Tiffany R. Walsh^{*a}

^aInstitute for Frontier Materials, Deakin University, Geelong, Vic. 3216, Australia

E-mail: tiffany.walsh@deakin.edu.au

Contents

- Figure S1 Snapshots of representative initial randomized arrangement of histidine adlayers at the graphene interface, in top view, (a) Neutral, (b) Zwitterion and (c) Mixed.
- Figure S2 Snapshots of representative initial randomized arrangement of alanine adlayers at the graphene interface, in top view, (a) Neutral, (b) Zwitterion and (c) Mixed.
- Figure S3 The structure of modelled amino acids used in this study, (a) histidine and (b) alanine. Pink dots indicate the reference atoms for the vertical density profile calculation.
- Figure S4 Snapshots of representative morphologies of the wet neutral zwitterion and mixed adlayers (top, histidine; bottom, alanine) on graphene surface (2×2 supercell). Graphene sheet is shown in grey, neutral and zwitterion amino acids are shown in blue and orange respectively. Red squares represent the simulation periodic boundaries. Green circles highlight incipient spontaneously-emerged ordered motifs.
- Figure S5 Quantification of exposed graphene surface. The 2D local density map of histidine atoms within (a) pure neutral, (b) pure zwitterion and (c) neutral-zwitterion mixed adlayers at dry and wet graphene interfaces.
- Figure S6 Quantification of exposed graphene surface. The 2D local density map of alanine atoms within (a) pure neutral, (b) pure zwitterion and (c) neutral-zwitterion mixed adlayers at dry and wet graphene interfaces.
- Figure S7 Percentage of the total number of molecules (200) in the first layer and second layer of the adsorbed adlayers at dry and wet graphene interfaces for (a) histidine and (b) alanine. First layer comprised amino acids located within 6.5 \AA ($C\alpha$ -graphene) from the graphene, whereas second layer contains amino acids located further than 6.5 \AA but within 13 \AA (C_a -graphene) of the graphene.
- Figure S8 Mixed adlayer compositional analysis (percentage population) in terms of neutral and zwitterionic species, analysed for layer one and layer two.
- Figure S9 Plan view zoomed in snapshots of representative spontaneously-emerged ordered motifs within pure zwitterion (a, c, and d) and mixed (b, e and f) histidine adlayers on dry (a and b) and wet (c, d, e and f) graphene surfaces. Surrounding amino acids in the layer are shown in translucent orange. Magenta arrows indicate position of C-terminus to imidazole ring.
- Figure S10 Plan view zoomed in snapshots of representative spontaneously-emerged ordered motifs within pure zwitterion (a, and b) and mixed (c and d) alanine adlayers on wet graphene surface. Surrounding amino acids in the layer are shown in translucent orange. Yellow arrows indicate directions of the N-termini to C-termini along the row.
- Figure S11 Side view zoomed in snapshots of representative spontaneously-emerged ordered row within zwitterion adlayers for alanine, showing the different orientations of the side-chain on the graphene surface.
- Figure S12 Plan view zoomed in snapshots of representative incipient ordered motifs within zwitterion (a, b, e and f) and mixed (c and d) adlayers for histidine (a, b, c and d) and alanine (e and f) at dry graphene interface, with annotations showing the measured size features within the motifs.
- Figure S13 2D radial density distribution functions (RDF) data related to inter-molecular distance. The 2D radial density distribution functions of $C\alpha$ - $C\alpha$ within the adlayers of histidine and alanine for the (a) pure, (b) mixed, dry and (c) mixed, wet cases. Only layer one molecules were considered. Dotted lines correspond to the inter-molecular spacing within the ordered motifs.
- Figure S14 2D radial density distribution functions (RDF) data related to the inter-molecular spacing. The 2D radial density distribution functions of the centre of ring within adlayers of histidine and $C_{\text{methyl}}-C_{\text{methyl}}$ within adlayers of alanine for the (a) pure, (b) mixed, dry and (c) mixed, wet cases. Only layer one molecules were considered. Dotted lines correspond to the inter-molecular spacing within the ordered motifs.
- Figure S15 Characterisation of water distribution on graphene surfaces. The 2D local density map of water atoms within (a) neutral, (b) zwitterion and (c) mixed histidine and alanine adlayers on graphene surfaces.
- Figure S16 Snapshots of representative hydrogen bonding configurations formed within adsorbed neutral histidine adlayers on the graphene surface. Hydrogen bonds shown in yellow colour. Surrounding histidines in the adlayer are shown in translucent orange.
- Figure S17 Snapshots of representative hydrogen bonding configurations formed within adsorbed zwitterion histidine adlayers on the graphene surface. Hydrogen bonds shown in yellow colour. Surrounding histidines in the adlayer are shown in translucent orange.
- Figure S18 Snapshots of representative hydrogen bonding configurations formed within adsorbed mixed histidine adlayers on the graphene surface. Hydrogen bonds shown in yellow colour. Surrounding histidines in the adlayer are shown in translucent orange.

- Figure S19 Snapshots of representative hydrogen bonding configurations formed within adsorbed neutral alanine adlayers on the graphene surface. Hydrogen bonds shown in yellow colour. Surrounding alanines in the adlayer are shown in translucent orange.
- Figure S20 Snapshots of representative hydrogen bonding configurations formed within adsorbed zwitterion alanine adlayers on the graphene surface. Hydrogen bonds shown in yellow colour. Surrounding alanines in the adlayer are shown in translucent orange.
- Figure S21 Snapshots of representative hydrogen bonding configurations formed within adsorbed mixed alanine adlayers on the graphene surface. Hydrogen bonds shown in yellow colour. Surrounding alanines in the adlayer are shown in translucent orange.
- Figure S22 Simulated annealing molecular dynamics simulation data showing the average number of inter-amino acid hydrogen bonds formed within the first layer of the adsorbed pure (a) and mixed (b and c) histidine adlayers on the graphene surface. N-N, Z-Z and N-Z represent neutral-neutral, zwitterion-zwitterion and neutral-zwitterion interactions respectively.
- Figure S23 Simulated annealing molecular dynamics simulation data showing the average number of inter-amino acid hydrogen bonds formed within the first layer of the adsorbed pure (a) and mixed (b and c) alanine adlayers on the graphene surface. N-N, Z-Z and N-Z represent neutral-neutral, zwitterion-zwitterion and neutral-zwitterion interactions respectively.
- Figure S24 Snapshots of representative water-amino acids hydrogen bonding configurations within the adsorbed histidine adlayers at wet graphene interface. Hydrogen bonds are shown in yellow colour. Surrounding histidines in adlayer and water are shown in translucent orange and blue respectively.
- Figure S25 Snapshots of representative water-amino acids hydrogen bonding configurations within the adsorbed alanine adlayers at wet graphene interface. Hydrogen bonds are shown in yellow colour. Surrounding alanines in adlayer and water are shown in translucent orange and blue respectively.
- Figure S26 Simulated annealing molecular dynamics simulation data showing the total number of water-amino acids hydrogen bonds formed within histidine and alanine adlayers at the wet graphene interface. N and Z represent hydrogen bonding within pure neutral and zwitterion adlayers respectively. N -M and Z -M represent water-neutral and water-zwitterion hydrogen bonding within the mixed adlayers respectively.
- Figure S27 Simulated annealing molecular dynamics (SAMD) simulation data showing the vertical density profiles with respect to the distance between (a) the center of histidine rings in the adlayers and graphene, and (b) the N term of alanine in the adlayers and graphene. (c) The probability distribution of the tilt angle between the histidine rings in the adlayers and the graphene surface, when the alpha-carbon (C_{α}) was within 6.5 Å of the graphene surface.
- Figure S28 Simulated annealing molecular dynamics (SAMD) simulation data showing the vertical density profiles with respect to the distance between neutral (a and b) and zwitterion (c and d) histidine and graphene for the adsorbed pure adlayers (a and c) and mixed mixed adlayers (b and d) on the graphene surface.
- Figure S29 Simulated annealing molecular dynamics (SAMD) simulation data showing the vertical density profiles with respect to the distance between neutral (a and b) and zwitterion (c and d) alanine and graphene for the adsorbed pure adlayers (a and c) and mixed a adlayers (b and d) on the graphene surface.
- Figure S30 Percentage contact of the total number of neutral and zwitterion molecules in the adsorbed (a) pure (200) and (b) mixed (100) adlayers at graphene interfaces. (c) Percentage contact for alanine's methyl side-chain with the graphene surface.
- Figure S31 The probability distributions of the tilt angle between the histidine rings in the adlayers and the graphene surface, when the alpha-carbon (C_{α}) was located further than 6.5 Å but within 13 Å (C_{α} -graphene) of the graphene surface.
- Figure S32 The probability distributions of the tilt angle between histidine rings in the staggered dimer row motif and the graphene surface.
- Figure S33 (a) Snapshots of representative morphologies of the wet neutral and zwitterion alanine adlayers with ion contaminants on graphene surface (2×2 supercell). (b) Snapshots of representative emergent ordered motifs within zwitterionic alanine adlayers with ion contaminants on wet graphene surface. Surrounding amino acids in the layer are shown in translucent orange.

Table S1 Average percentages of exposed graphene surface, for the different amino acid adlayers.

Table S2 Total number of water-water hydrogen bonds within the different adlayers of histidine and alanine adsorbed on wet graphene surface.

Table S3 Averaged structural properties of neutral amino acids calculated from simulated annealing molecular dynamics (SAMD). Interfacial separation distances, dsep (Å), between neutral histidines and alanines in the adsorbed adlayer and graphene, and tilt angle between aromatic ring and graphene surface. Where applicable, two numbers indicate the position of pronounced peak one and two respectively.

Table S4 Averaged structural properties of zwitterion amino acids calculated from simulated annealing molecular dynamics (SAMD). Interfacial separation distances, dsep (Å), between zwitterionic histidines and alanines in the adsorbed adlayer and graphene, and tilt angle between aromatic ring and graphene surface. Where applicable, two numbers indicate the position of pronounced peak one and two respectively.

Videos Description

The videos **Ala-Z-graphene** and **Ala-NZ-graphene** show the molecular dynamic simulations of the spontaneous emergence of patterns co-existing in purely zwitterionic and neutral-zwitterionic mixture alanine adlayers, respectively, on graphene *in vacuo* from an initially randomised arrangement. Video **Ala-N-graphene** shows the molecular dynamic simulations disordered purely neutral adlayer of alanine on graphene in vacuo from an initially randomised arrangement. Graphene sheet is shown in grey, neutral and zwitterion amino acids are shown in blue and orange respectively.

Computational Methods: Details of Analyses

All analyses of the amino acid adlayers were carried out using trajectories obtained from the aggregation of the last 300 frames from the final phase of each of the five simulated annealing cycles. Unless stated otherwise, all data presented herein were averaged over the independent simulations. In this study, we calculated the percentage of exposed graphene surface upon adsorption of adlayers as a quantitative probe of the adlayer surface coverage, using 2D local density maps of the amino acid atoms. We characterised the adlayers morphologies by calculating the percentages of molecules residing in the different layers within the adlayers. The percentage of total molecules in first and second layer of adsorbed adlayers and percentage of amino acid species in first and second layers were determined, using a 6.5 Å cutoff for the interfacial separation distance between alpha-carbon (C_α) with respect to the graphene. The morphologies of trace water in the adsorbed adlayers on graphene (for the wet interfaces) were determined *via* 2D local density map of the water atoms and degree of water-water hydrogen bonding interactions. Inter-molecular hydrogen bonding analyses were also performed to determine the degree of inter-amino acid and water-amino acid hydrogen bonding interactions within the adsorbed adlayers. Additionally, the interfacial separation distance between the amino acids in the adlayers and graphene, with respect to the reference sites indicated in Figure S3, were determined using number densities profiles. The tilt angle between the imidazole rings of histidine in the adlayer and the graphene surface was calculated to determine the orientation of the His ring on graphene. The degree of amino acid-graphene contact was characterised by calculating the percentage of the total number of each amino acid state in the adlayers found within a cut-off distance with respect to graphene. The reference site in His for the surface contact calculation was the centre of the aromatic ring and the cut-off distance used was ~ 4.5 Å, based on inspection of the vertical density profiles. For Ala, the degree of amino acid-graphene contact was calculated with respect to both amine group N and C_{methyl} . The cut-off distances used for the amine-surface and C_{methyl} -surface contacts were ~ 4 Å and ~ 4.5 Å, respectively. These cut-off distances were chosen based on inspection of the vertical density profiles. For a fuller description of how these analyses were performed, the authors refer the readers to the previous studies of Awuah and Walsh.¹

Further details of Results and Discussion:

Adlayer Morphology

To further characterise the morphologies and determine the vertical organisation of the amino acids, we quantified the proportion of the amino acids in the different layers within the morphologies (provided in Fig. S7 and S8). We found that the adsorbed zwitterion and mixed adlayer morphologies were composed of mostly two layers, whereas the neutral adlayer morphologies comprised only one layer, indicating that the presence of zwitterions in the adlayers induced multi-layer formation. In addition, for both amino acids, the percentage population of neutral species (~48%) in the first layer of the mixed adlayers were comparable to that of zwitterionic species. The second layer of Ala comprised ~57% of neutral species and ~43% of zwitterions. In contrast, the percentage population of neutral states (~79%) in the second layer of mixed His adlayers was relatively greater than that of zwitterions (~21%).

Dimers and Trimers

Specifically, at the dry graphene interface, Ala pure neutral (Ala-N) adlayers revealed relatively higher percentage population of dimer (~ 30 % of total number of adsorbed molecules) and trimer (~ 22 %) units compared to His-N adlayers (~8 % and ~4 % for dimer and trimer units respectively). The high percentage of discrete dimer and trimer units in the Ala-N adlayer can be explained by the fact that the methyl side-chain has no capacity to support inter-molecular hydrogen bonding, and as such all interactions are mostly formed between the C-terminus-C-terminus pairs. In comparing the population of the discrete dimer units of His and Ala to that of Trp and Met (determined from previous work¹), the order of the four amino acids with the highest percentage was found to be Ala > Trp > Met > His, indicating that His-N may not prefer C-terminus/C-terminus interactions in the neutral adlayer.

Additional Characterisation

To check that molecular ordering was actually incipient in the adlayers and to capture feature sizes within the structures, we calculated the inter-molecular 2D RDFs, described in the ESI section below, with reference to the C_α of the amino acids, and the centre of ring and C_{methyl} of His and Ala, respectively in the first adsorbed layers. Our 2D RDF calculations reflected the emergence of ordered motifs in the zwitterion-containing adlayers, and also confirmed the feature sizes within the structures (Fig. S13 and S14).

In terms of the effect of the trace water on the spontaneously-emergent motifs within the amino acid adlayers, we observed a similar trend as previously reported for Trp and Met adlayers. Specifically, the presence of the trace water neither induced nor disrupted the formation of the ordered motifs.¹ However, as detailed below, the percentage population of discrete dimer and trimer units within the neutral adlayers was reduced in the presence of trace water. Additionally, the morphologies of the trace water within the amino acid adlayers were characterised based on visual inspection and 2D local density maps of the water atoms

(Fig. S15) and quantification of water-water interactions (summarised in Table S2). These data were consistent with previous simulations of Trp and Met adlayers at the wet graphene interface (ESI section herein, 'Trace Water Morphology and Effects').

We also examined the effect of the side-chain characteristics on the adsorption geometries of the individual molecules within the adlayers. Full details of the surface-molecule vertical density profiles, ring tilt angle and ring-surface contacts of His, and amine-surface, and methyl-surface contacts of Ala are provided in section 'Individual Molecules within Adlayers', provided herein. In summary, we found that the adsorption geometries of the individual molecules in the adlayers were influenced by the side-chain characteristics, consistent with previous studies of single isolated His and Ala on the graphene surface. We also found that the overall trends in the effect of the termination state and trace water on the individual adsorption geometries reflected that of Trp and Met on graphene.¹

2D RDF distribution functions

For each adlayer/graphene system, we calculated 2D radial distribution functions (RDFs) with respect to the C_α of the amino acids, centre of His ring and C_{methyl} of Ala to check for lateral ordering and feature sizes within the first layer (i.e. within a distance of 6 Å) of the adsorbed adlayers on graphene (See details in Ref 1). As provided in Figure S13 and Figure S14, there was substantial evidence of longer-scale ordering (~25 Å) in the zwitterion-containing adlayers, supporting the findings of our visual inspection. In addition, the measured feature sizes (inter-molecular spacing) in the ordered structures from our trajectories (Figure S12) were captured by our calculated 2D RDF.

Trace water morphology and effects

Figure S4 provides snapshots of representative morphologies of the adlayers for the wet graphene interface. The 2D local density map of the water atoms and water-water interactions are provided in Figure S15 and Table S2, respectively. Based on these data, we found that the trace water was distributed throughout the zwitterion-containing adlayers, whereas, the trace water mostly clustered to form nanodroplets in the neutral adlayers. The clustering was as a result of the relatively higher number of inter-molecular interactions between the trace water, as indicated in Table S2. These data were found consistent to that of Trp and Met adlayers on graphene.¹

Regarding the effect of the trace water on the amino acid morphologies, we noted that spontaneously-emergent motifs were present at the wet interface (Figures S9 and S10), indicating that the trace water did not disrupt the formation of the motifs. However, in the neutral adlayers, we found a reduction in the percentage population of the dimer (~20 % for Ala and ~4 % for His) and trimer (~15 % for Ala and ~2 % for His) units for the amino acids, especially for Ala. This reduction can be linked to the disruption of molecule-molecule interactions by the presence of the trace water, which was certainly expected per previous work.¹ In addition, the overall trends in the effect of the trace water on the layer compositions reflected that of Trp and Met¹. In summary, the composition of the zwitterion species in the second layer was increased, especially in the mixed adlayers.

Individual molecules within adlayers

Here, the influence of the side-chain characteristics on the adsorption mode of the individual molecules within the adlayers was determined. These data were obtained from the number density profiles of the adsorbed adlayers as a function of vertical distance from graphene, summarised in Figure S27 (See Figures S28 and S29 for details of number density profiles). In addition, the calculated numerical values of the interfacial separation distances between the adsorbed amino acid in the adlayers and graphene are provided in Tables S3 and S4. Our data showed that His interacts with graphene surface chiefly *via* the aromatic ring, irrespective of the termination state, at an average distance of ~ 3.7 Å. This was consistent with the adsorption mode of tryptophan (Trp) on graphene, however, the Trp ring was found relatively closer to the graphene (~ 3.4 Å).¹ For Ala, we found that the amine group maintained a close contact with graphene (~ 3.3 Å), as a result of the absence of an aromatic side-chain. A similar finding was reported by Awuah and Walsh for methionine (Met) adlayers at graphene interface.¹ Nonetheless, in the case of the adsorbed Met adlayers, the presence of an extended S-methyl thioether side-chain ensured a more direct contact with graphene via sulphur, compared with the amine group.¹ Based on our calculated separation distance for Ala, we also noted that methyl side-chain was mostly located at either ~ 3.5 Å or ~ 5.3 Å (where applicable) above the graphene surface. This suggests that the side-chain of adsorb Ala can assume several orientations on graphene (Figure S11), which can be linked to a subtle competition involving the methyl side-chain in Ala. Similar to previous studies, we found that the terminate state does not substantially affect the adsorption distances of the amino acid adlayers.¹ However, our data clearly suggest that the different characteristics of amino acid side-chains can influence the adsorption mode of the amino acid adlayers on graphene. This is comparable to several theoretical studies of amino acids on graphene.¹⁻⁵

In comparing the density profiles of the different amino acid states, the overall trends in the effect of the termination state reflected that of Trp and Met adlayers on graphene.¹ Generally, we found that the peak heights of the density profiles of adlayers comprising *pure* neutral amino acids were relatively higher compared to that of *pure* zwitterion amino acids, indicating that more neutral amino acids were in direct contact with the dry graphene surface than zwitterion amino acids.¹ In the mixed adlayers, we also found the trends in the peak heights of the density profiles broadly agreed with that of the pure adlayers, as shown in Figure S27. We further quantified the His and Ala molecules in close contact with the graphene. This was determined by calculating the ring-surface of His and amine-surface contacts of Ala for both species (Figures S30a and b). Consistent to that of Trp and Met adlayers, our data showed that there were relatively more neutral species in direct contact with graphene compared to the zwitterions, especially in the pure adlayers. This can be attributed to the vertical molecule-molecule stacking induced by the zwitterions, which supported our proposed mechanism for single- and multi-layered organisation of amino acid adlayers reported in previous studies.¹ In the case of Ala, we further characterised the degree of methyl side-chain-graphene contact, revealing that there were relatively more zwitterionic species with their side-chains in direct contact with graphene than the neutral species, as shown in Figure S30c. That said, we noted that relatively more His rings were in direct contact with graphene than the methyl side-chain in Ala. On the basis of these data, we believe the methyl side-chain in Ala weakly engages with graphene compared to the imidazole ring in His.

For His adlayers, the orientation of the aromatic rings was also analyzed. The probability distributions of the tilt angle between the rings and the graphene surface, when the molecules

are located within the first layer of the adlayers are provided in Figure S27c. Our data showed that the ring in His can align in a broad range of orientations on graphene, with a relatively higher probability of near-planar orientations. Nonetheless, in comparing this data to that of Trp, we found that Trp rings featured relatively higher probability of near-planar orientations with respect to graphene surface than His.¹ A similar finding was reported by Hughes *et al.* for adsorption of isolated Trp and His at aqueous graphene interface.² Similar to Trp adlayers, we found that the His rings within the second layer of the adlayers (where applicable) showed no preferred ring configuration on graphene (Figure S31).

In comparing the surface contacts and tilt angle distributions (where applicable) obtained at wet graphene interface to that of the dry interface, we noted that the overall trends in surface contact distance and ring orientation were broadly comparable to that of Trp and Met.¹ In particular, for the *pure* adlayers, the His ring-surface and Ala amine-surface contacts of the neutral states on graphene were mildly affected by presence of trace water, whereas that of the zwitterion states were reduced, especially for Ala (Figures S19(a and b)). However, in the mixed adlayers, while the surface contacts for both His species (His-N and His-Z) were almost unaffected by the presence of trace water, the amine-surface contacts for the zwitterion Ala (Ala-Z) showed a substantial reduction. Moreover, for both Ala-N and Ala-Z in the pure and mixed adlayers, the methyl-surface contacts were mildly affected by the presence of the trace water (Figure S30c).

With regards to the orientation of the His rings on graphene in the presence of trace water, we noted that the overall alignment did not change. However, similar to the Trp-Z ring, the probability of His-Z ring with near-planar configuration was enhanced by the presence of trace water in the adlayers. This suggests that the presence of trace water enhances the parallel geometry of zwitterion His on graphene. In the case of His-N, the probability distributions of the ring were mostly unaffected by the trace water. Overall, our simulation data show that while the termination state did not adversely affect the molecule-graphene interfacial separation distances, the side-chain characteristics influenced the adsorption mode of the AA adlayers. In addition, the presence of trace water had no drastic effect on the adsorption mode of the AA adlayers on graphene but had substantial impact on the adsorption geometries of the zwitterions.

References

- 1 J. B. Awuah and T. R. Walsh, *Small*, 2020, **16**, 1–11.
- 2 Z. E. Hughes, S. M. Tomásio and T. R. Walsh, *Nanoscale*, 2014, **6**, 5438–5448.
- 3 C. Rajesh, C. Majumder, H. Mizuseki and Y. Kawazoe, *J. Chem. Phys.*, 2009, **130**, 124911.
- 4 H. Vovusha, S. Sanyal and B. Sanyal, *J. Phys. Chem. Lett.*, 2013, **4**, 3710–3718.
- 5 R. Zhiani, *Appl. Surf. Sci.*, 2017, **409**, 35–44.

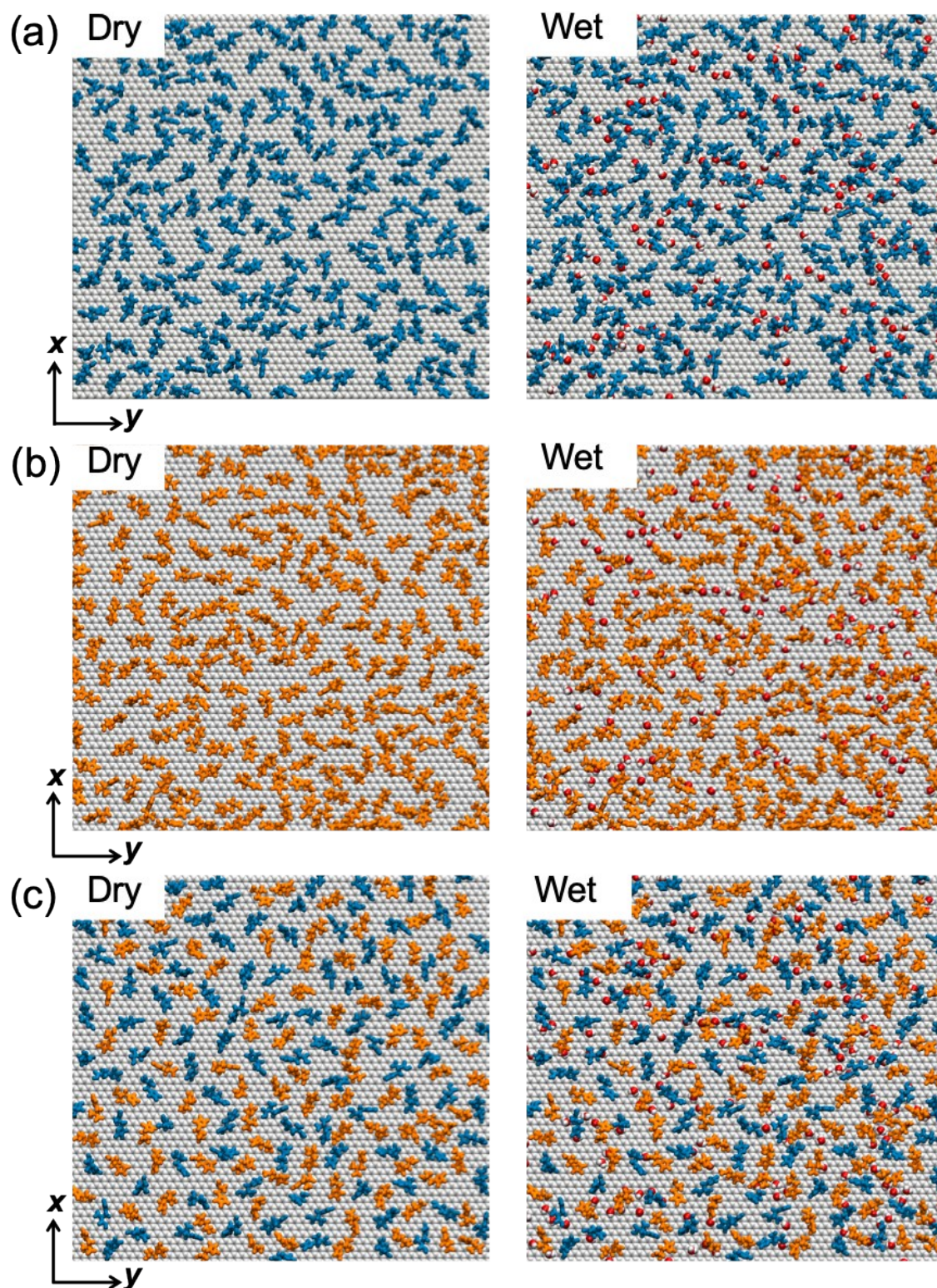


Figure S1 Snapshots of representative initial randomized arrangement of histidine adlayers at the graphene interface, in top view, (a) Neutral, (b) Zwitterion and (c) Mixed.

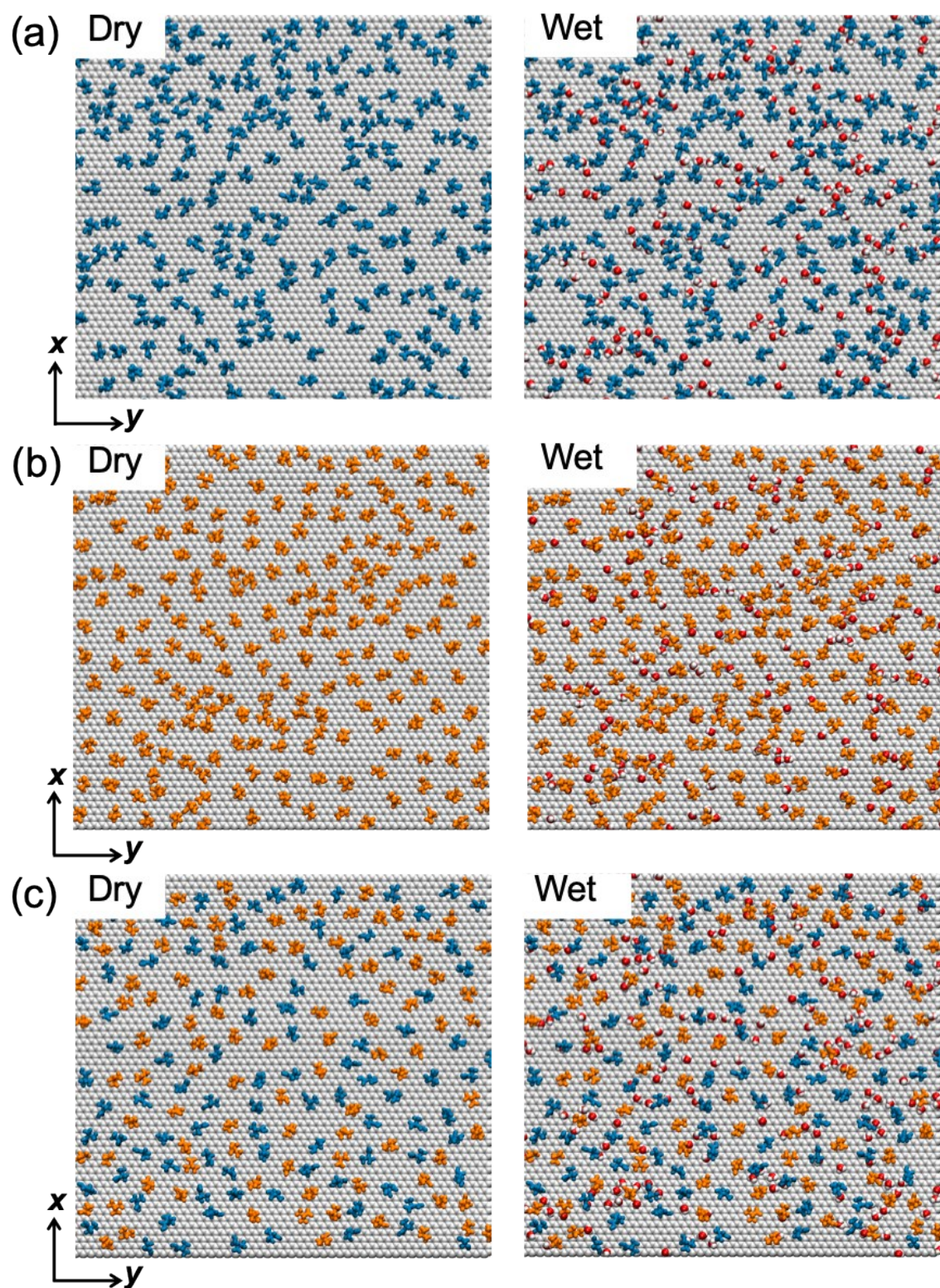


Figure S2 Snapshots of representative initial randomized arrangement of alanine adlayers at the graphene interface, in top view, (a) Neutral, (b) Zwitterion and (c) Mixed.

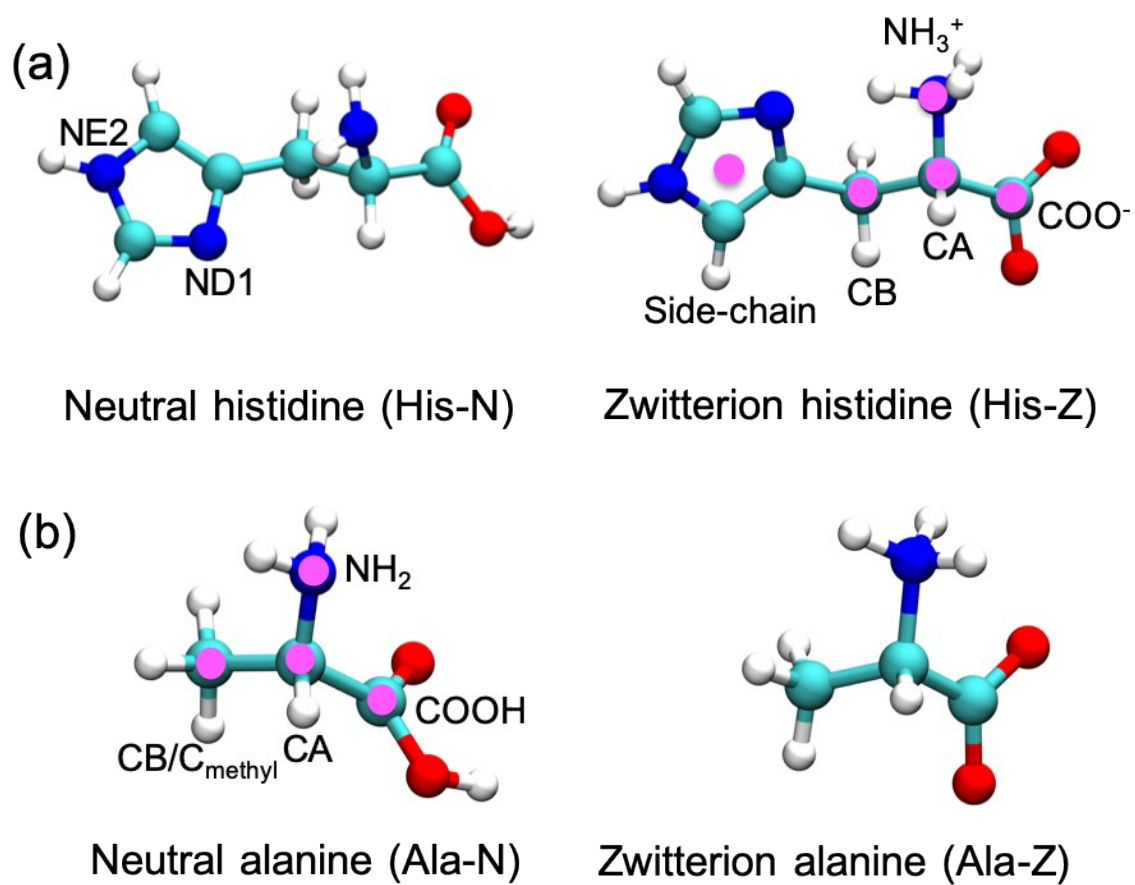


Figure S3 The structure of modelled amino acids used in this study, (a) histidine and (b) alanine. Pink dots indicate the reference atoms for the vertical density profile calculation.

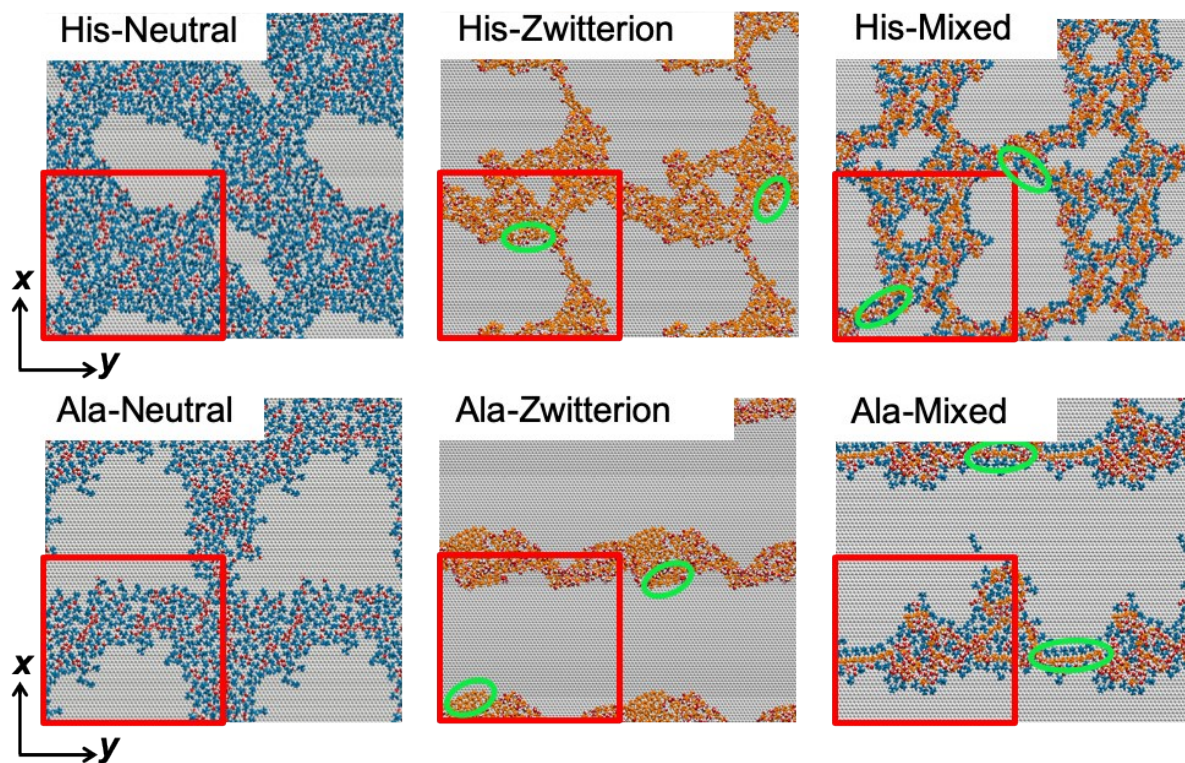


Figure S4 Snapshots of representative morphologies of the wet neutral zwitterion and mixed adlayers (top, histidine; bottom, alanine) on graphene surface (2×2 supercell). Graphene sheet is shown in grey, neutral and zwitterion amino acids are shown in blue and orange respectively. Red squares represent the simulation periodic boundaries. Green circles highlight incipient spontaneously-emerged ordered motifs.

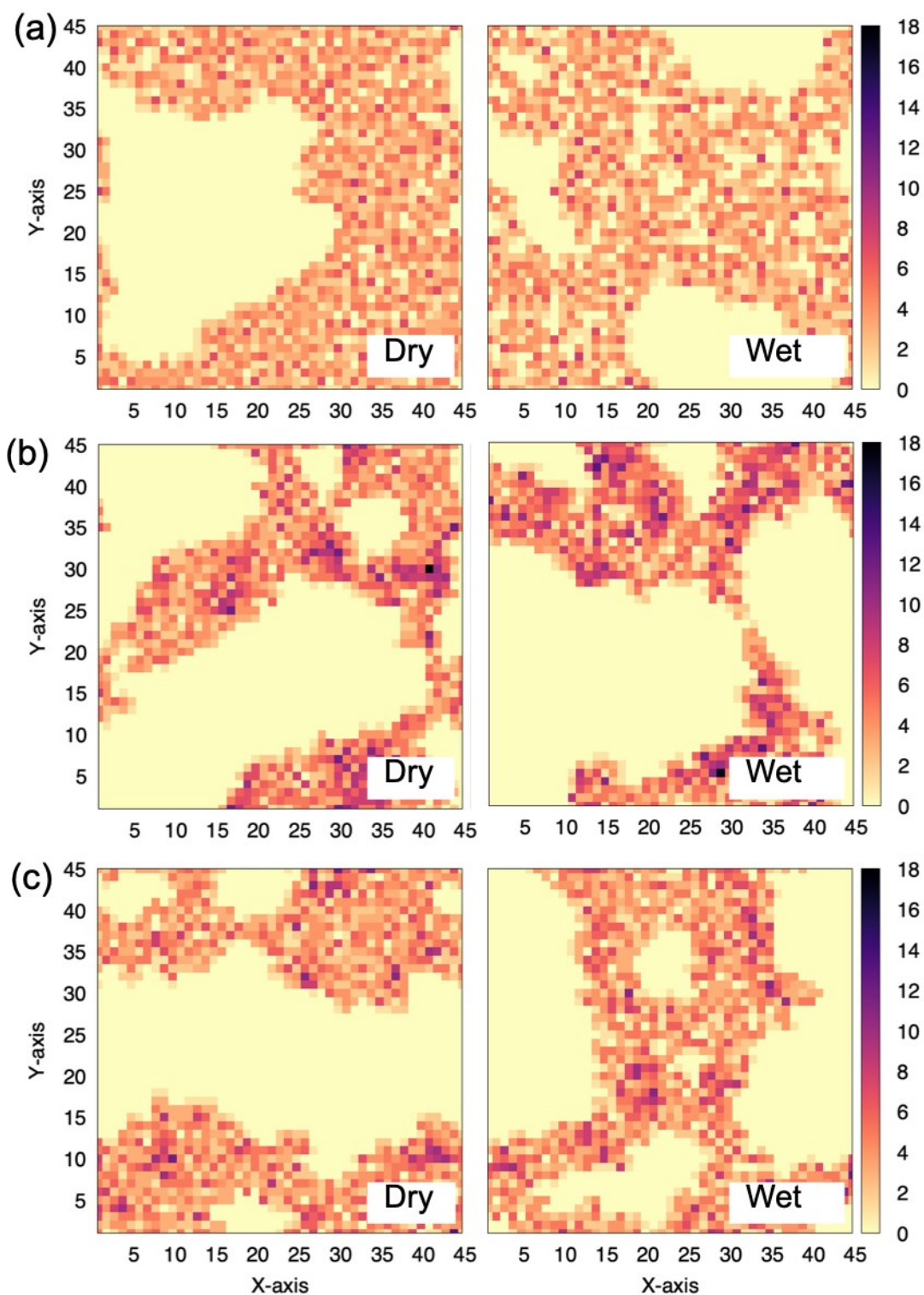


Figure S5 Quantification of exposed graphene surface. The 2D local density map of histidine atoms within (a) pure neutral, (b) pure zwitterion and (c) neutral-zwitterion mixed adlayers at dry and wet graphene interfaces.

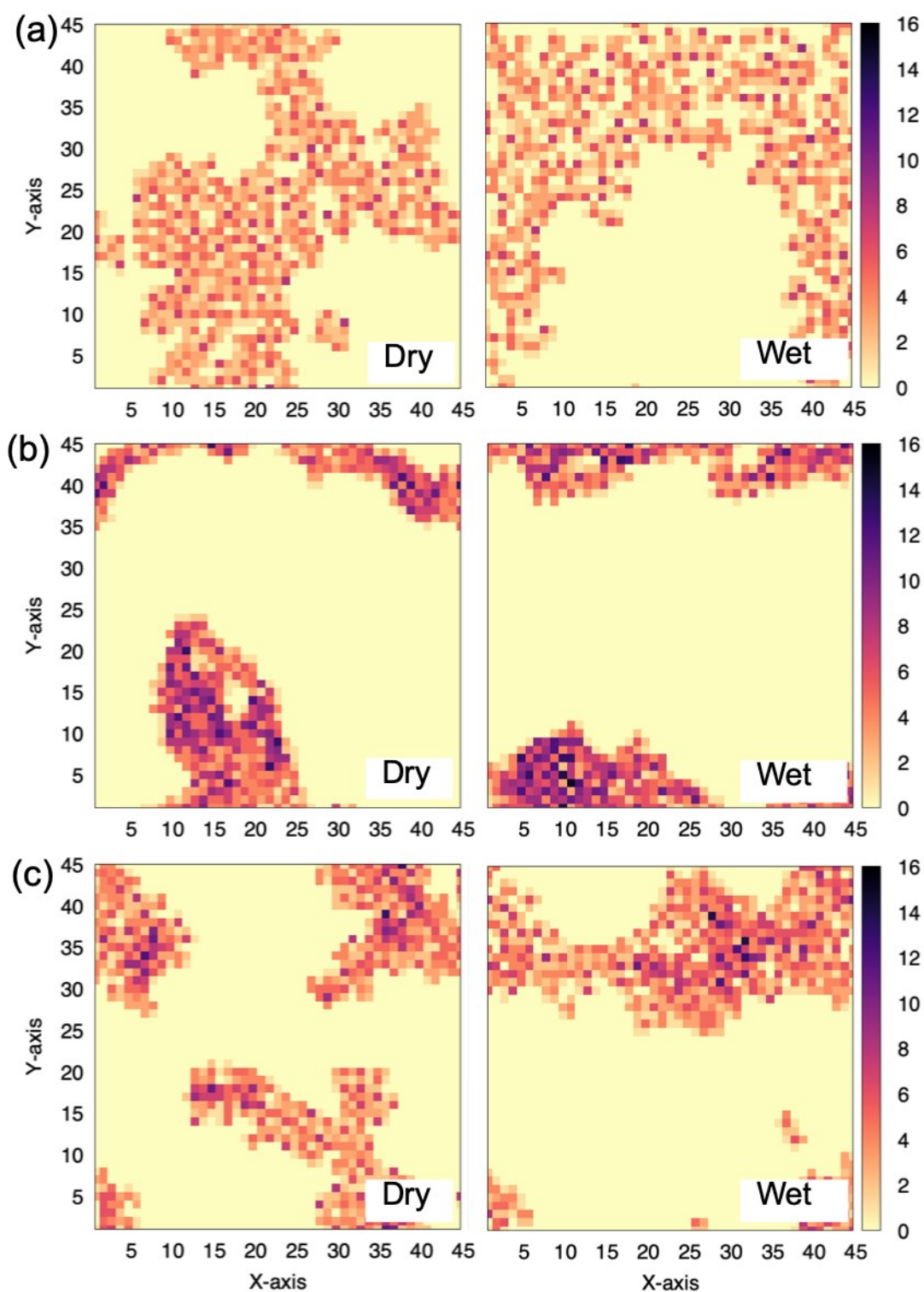


Figure S6 Quantification of exposed graphene surface. The 2D local density map of alanine atoms within (a) pure neutral, (b) pure zwitterion and (c) neutral-zwitterion mixed adlayers at dry and wet graphene interfaces.

Table S1 Average percentages of exposed graphene surface, for the different amino acid adlayers.

System	Percentage (%)	
	Dry	Wet
His-N	37	35
His-Z	51	57
His-mixed	45	48
Ala-N	57	54
Ala-Z	75	73
Ala-mixed	64	65

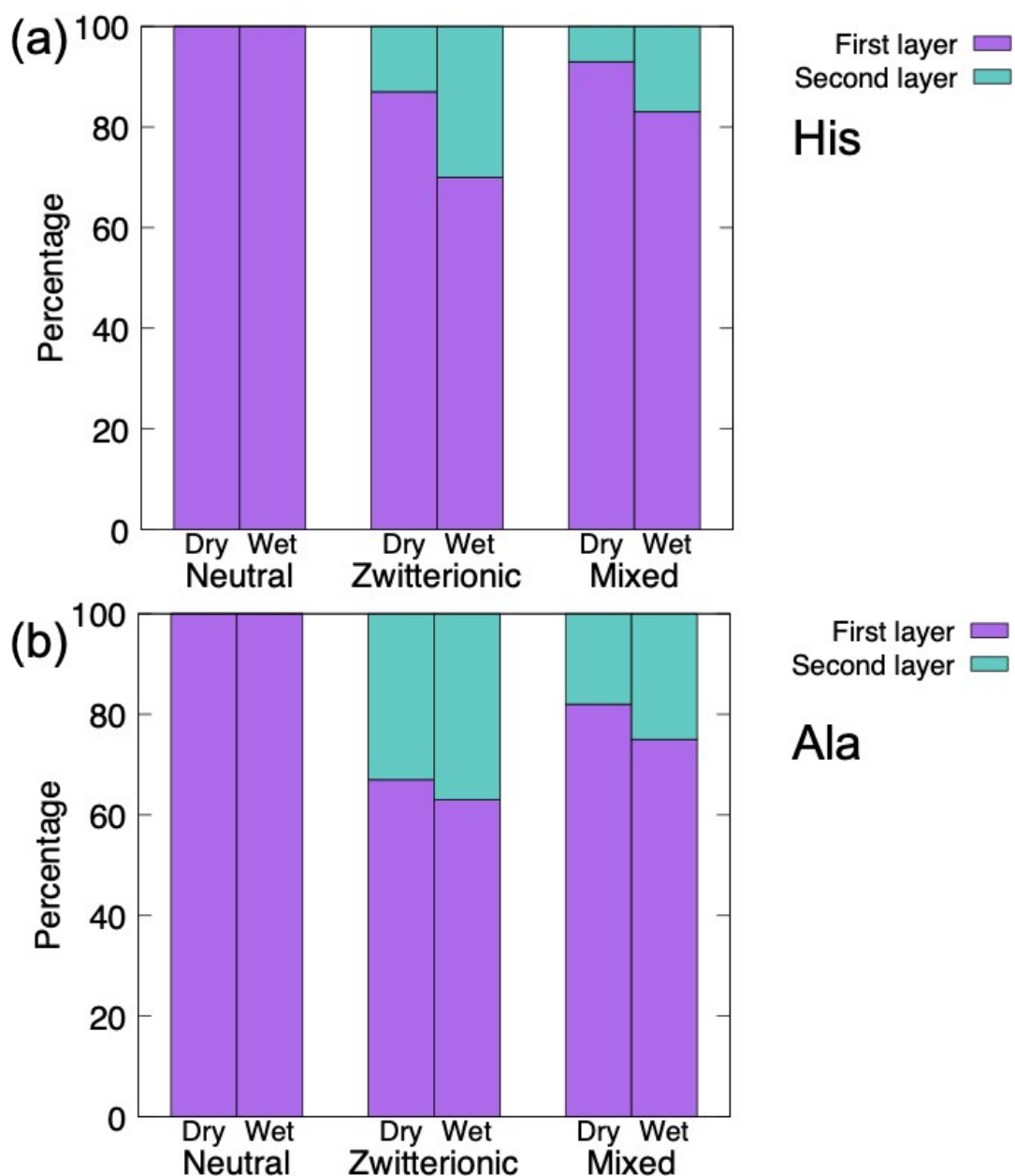


Figure S7 Percentage of the total number of molecules (200) in the first layer and second layer of the adsorbed adlayers at dry and wet graphene interfaces for (a) histidine and (b) alanine. First layer comprised amino acids located within 6.5 Å (C_{α} -graphene) from the graphene, whereas second layer contains amino acids located further than 6.5 Å but within 13 Å (C_{α} -graphene) of the graphene.

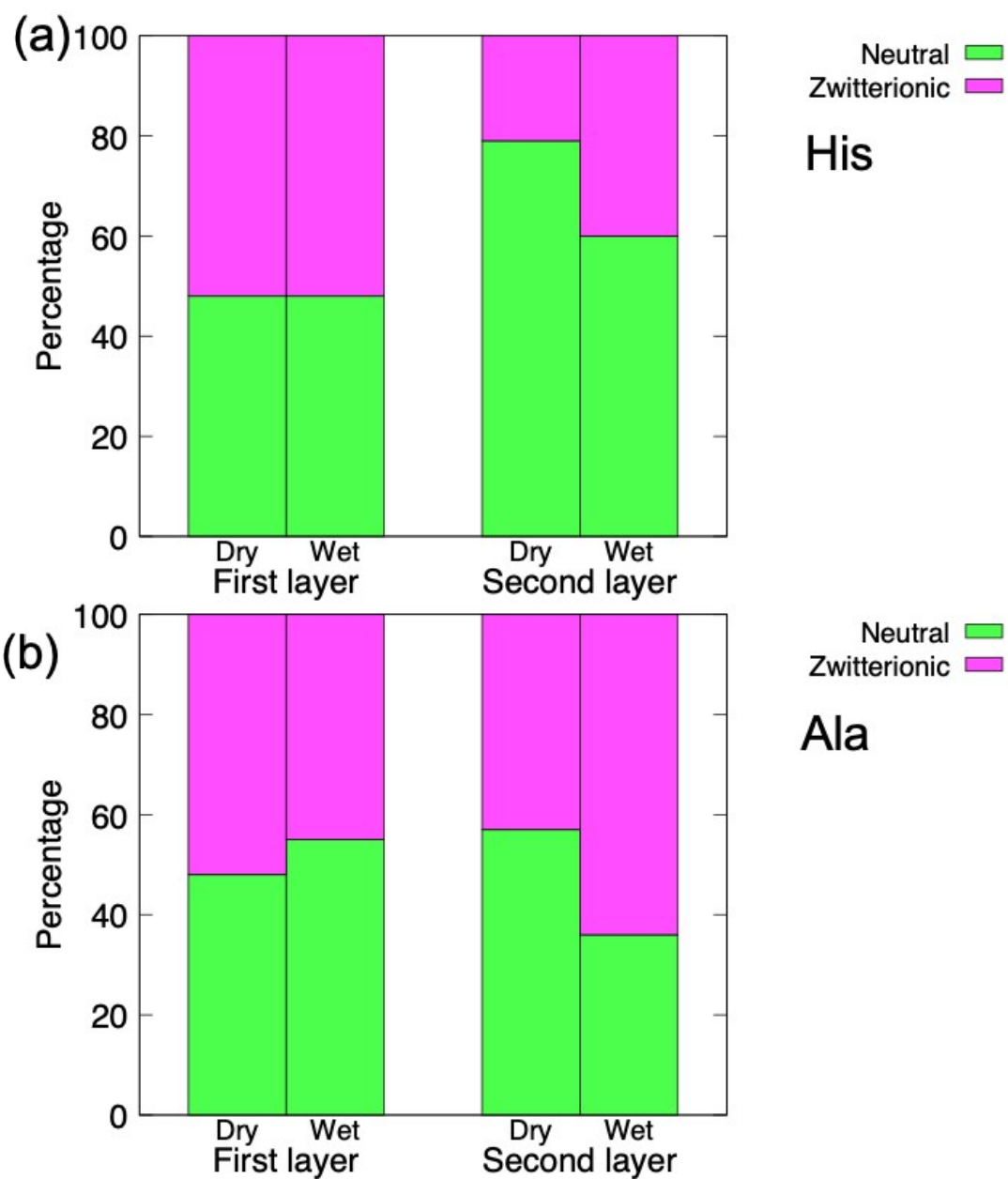


Figure S8 Mixed adlayer compositional analysis (percentage population) in terms of neutral and zwitterionic species, analysed for layer one and layer two.

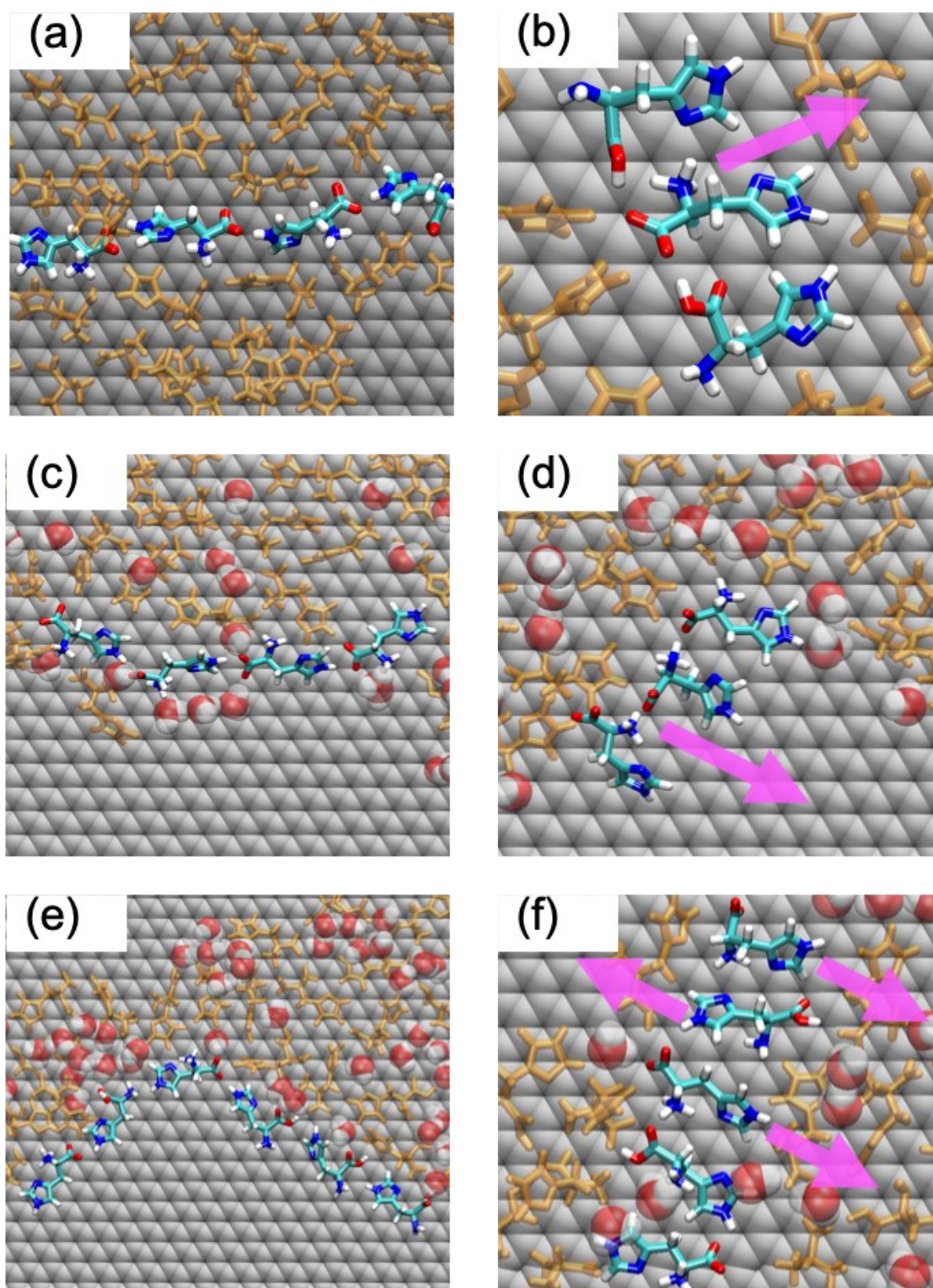


Figure S9 Plan view zoomed in snapshots of representative spontaneously-emerged ordered motifs within pure zwitterion (a, c, and d) and mixed (b, e and f) histidine adlayers on dry (a and b) and wet (c, d, e and f) graphene surfaces. Surrounding amino acids in the layer are shown in translucent orange. Magenta arrows indicate position of C-terminus to imidazole ring.

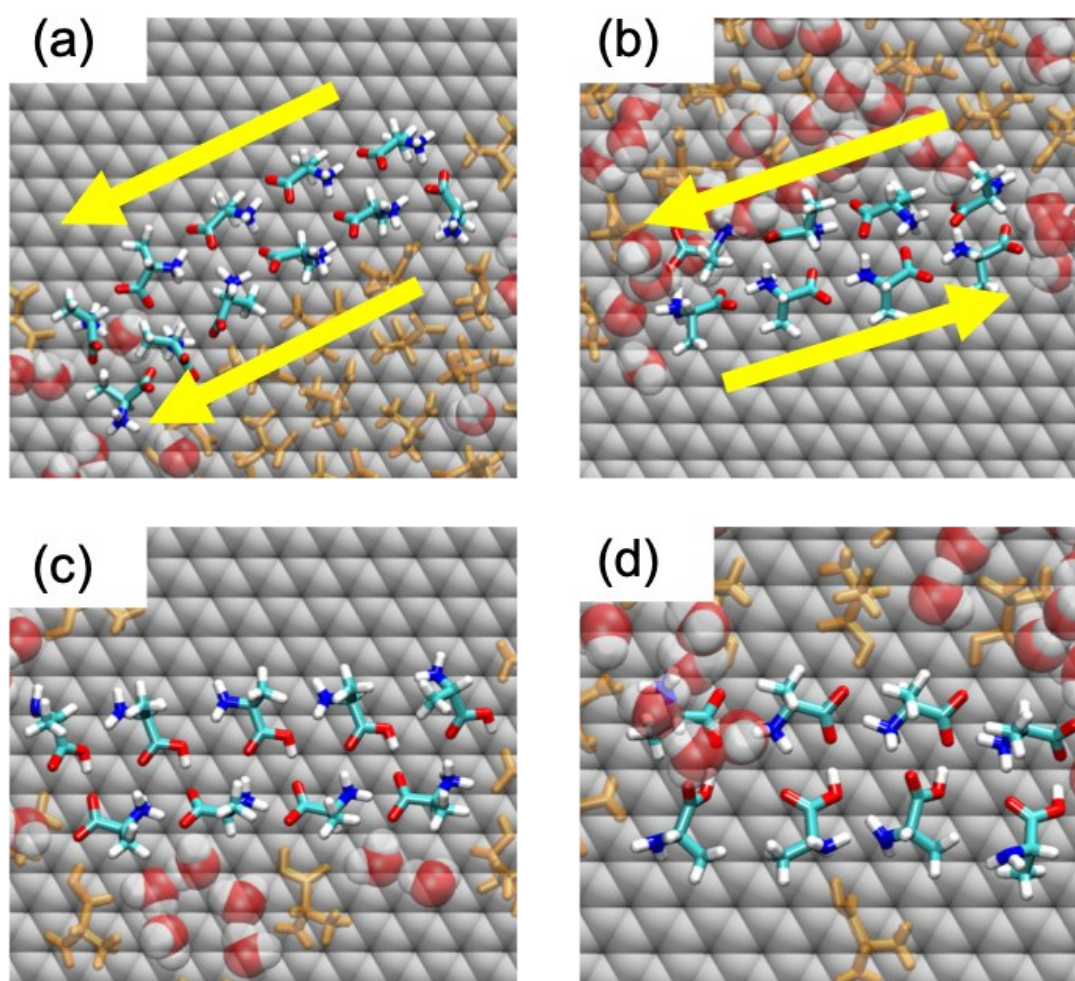


Figure S10 Plan view zoomed in snapshots of representative spontaneously-emerged ordered motifs within pure zwitterion (a, and b) and mixed (c and d) alanine adlayers on wet graphene surface. Surrounding amino acids in the layer are shown in translucent orange. Yellow arrows indicate directions of the N-termini to C-termini along the row.

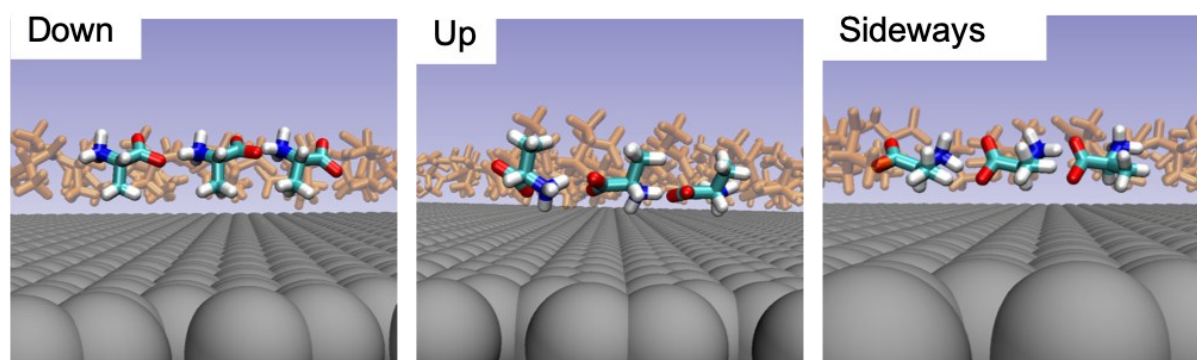


Figure S11 Side view zoomed in snapshots of representative spontaneously-emerged ordered row within zwitterion adlayers for alanine, showing the different orientations of the side-chain on the graphene surface.

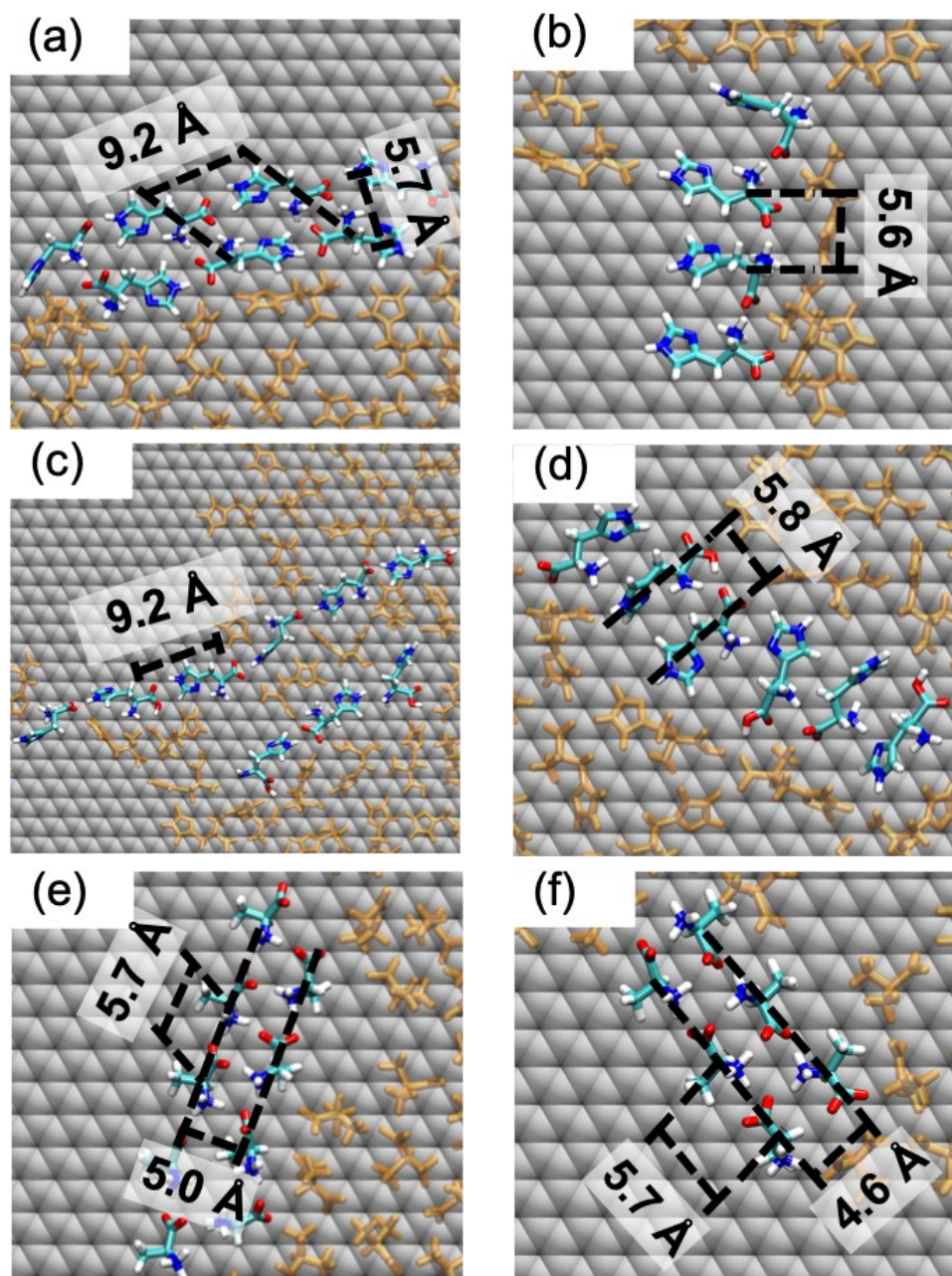


Figure S12 Plan view zoomed in snapshots of representative incipient ordered motifs within zwitterion (a, b, e and f) and mixed (c and d) adlayers for histidine (a, b, c and d) and alanine (e and f) at dry graphene interface, with annotations showing the measured size features within the motifs.

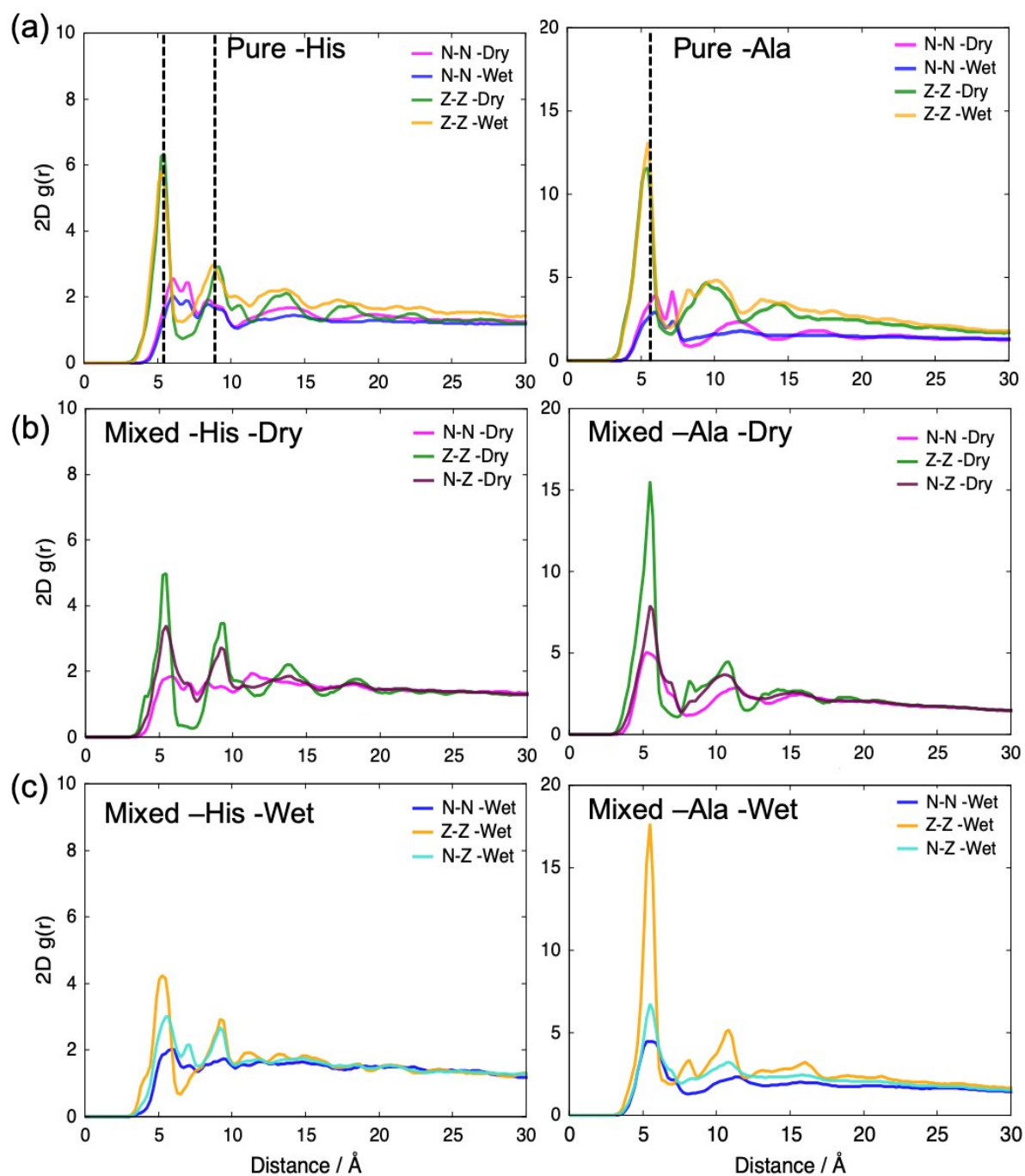


Figure S13 2D radial density distribution functions (RDF) data related to inter-molecular distance. The 2D radial density distribution functions of $C\alpha$ - $C\alpha$ within the adlayers of histidine and alanine for the (a) pure, (b) mixed, dry and (c) mixed, wet cases. Only layer one molecules were considered. Dotted lines correspond to the inter-molecular spacing within the ordered motifs.

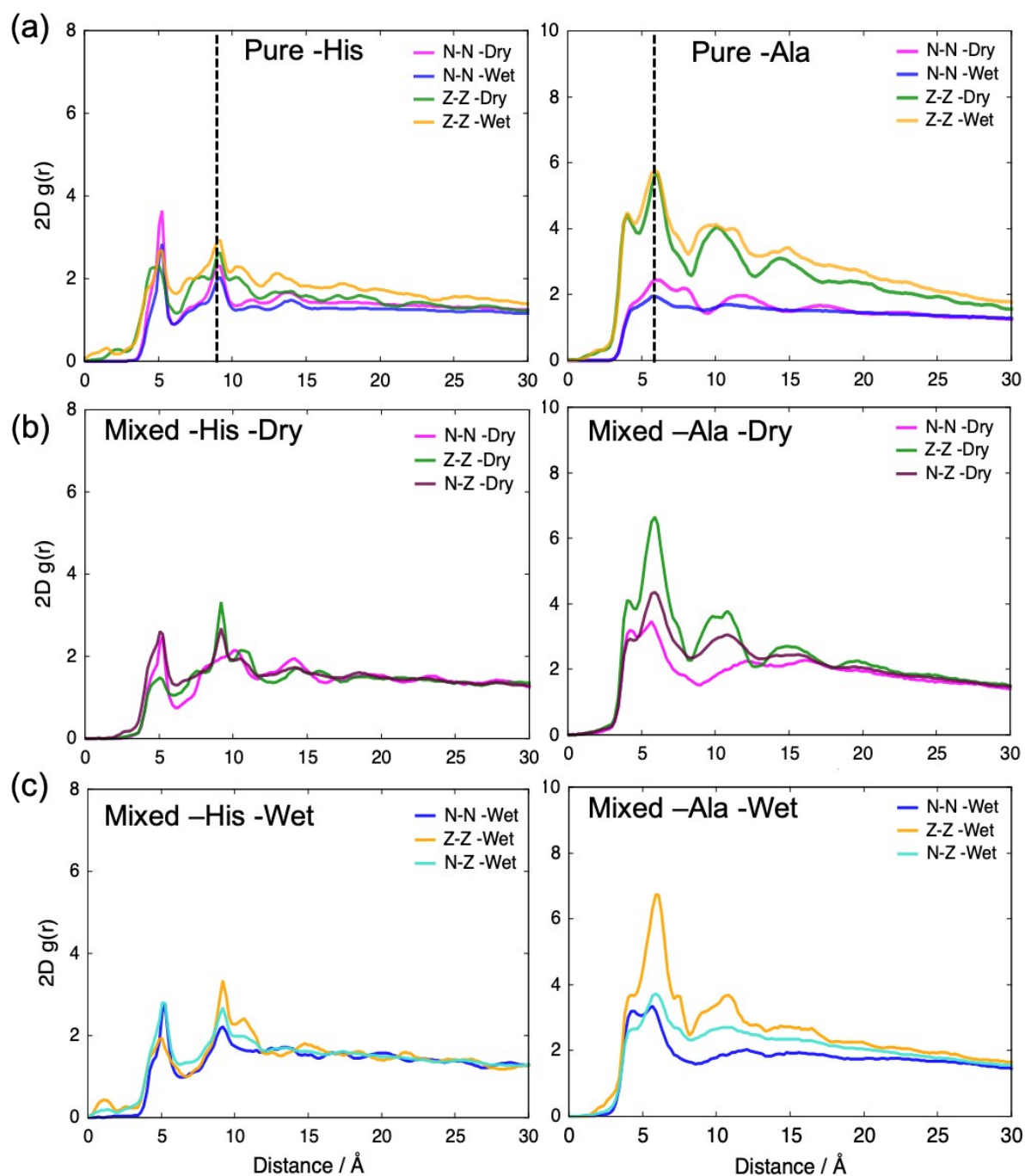


Figure S14 2D radial density distribution functions (RDF) data related to the inter-molecular spacing. The 2D radial density distribution functions of the centre of ring within adlayers of histidine and $C_{\text{methyl}}-C_{\text{methyl}}$ within adlayers of alanine for the (a) pure, (b) mixed, dry and (c) mixed, wet cases. Only layer one molecules were considered. Dotted lines correspond to the inter-molecular spacing within the ordered motifs.

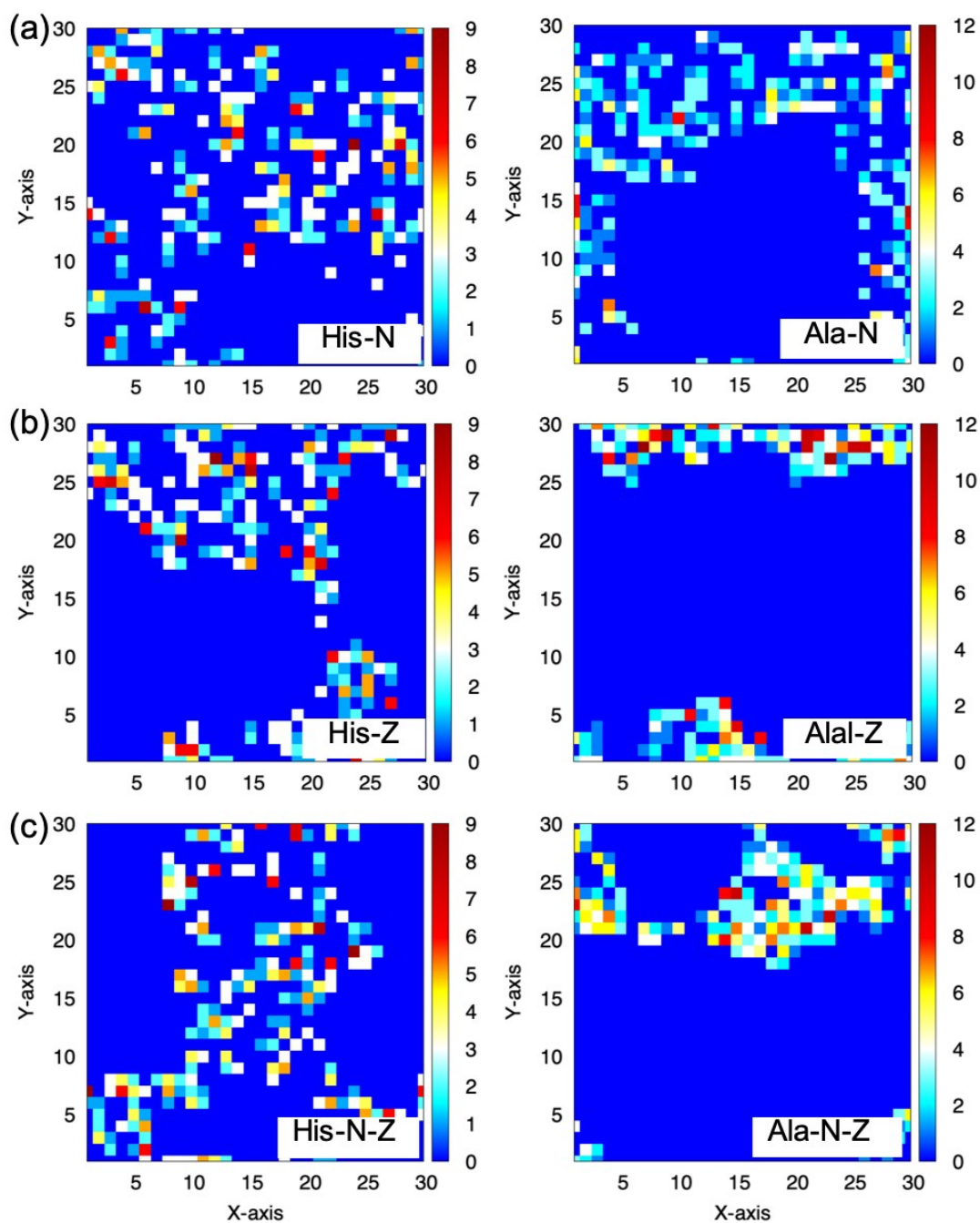
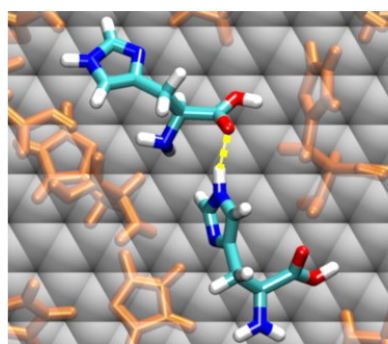


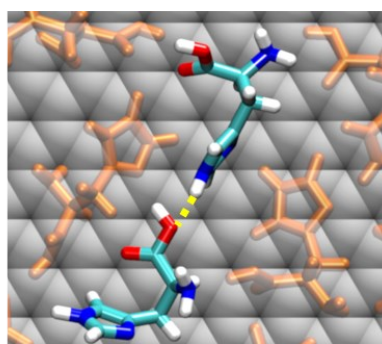
Figure S15 Characterisation of water distribution on graphene surfaces. The 2D local density map of water atoms within (a) neutral, (b) zwitterion and (c) mixed histidine and alanine adlayers on graphene surfaces.

Table S2 Total number of water-water hydrogen bonds within the different adlayers of histidine and alanine adsorbed on wet graphene surface.

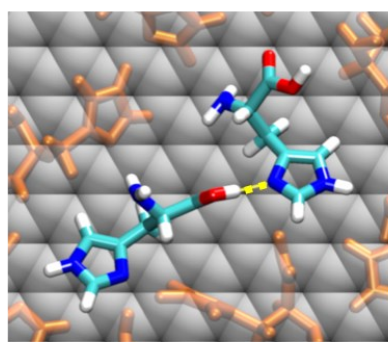
System	Number of H-bonds	
	His	Ala
Neutral	100.6±5.8	108.8±6.6
Zwitterion	53.2±3.2	88.3±8.6
Mixed	59.9±3.8	97.4±4.6



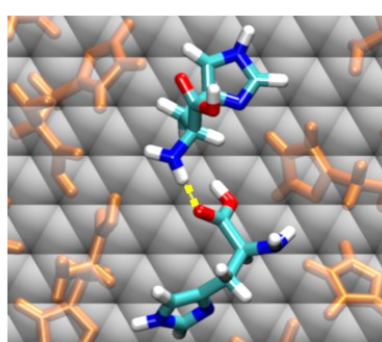
OT1-HE2-NE2 (C term-Ring)



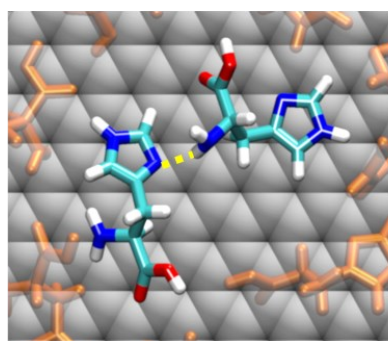
OT2-HE2-NE2 (C term-Ring)



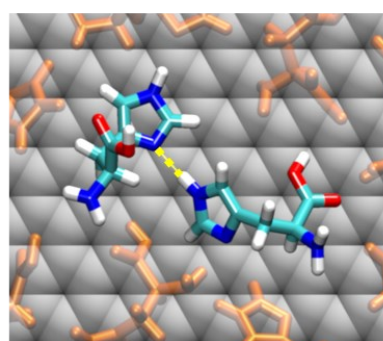
ND1-H-OT2 (C term-Ring)



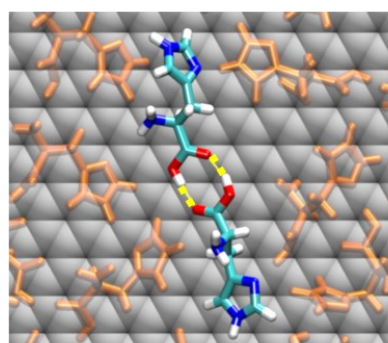
OT1-HT-N (C term-N term)



ND1-HT-N (Ring-N term)

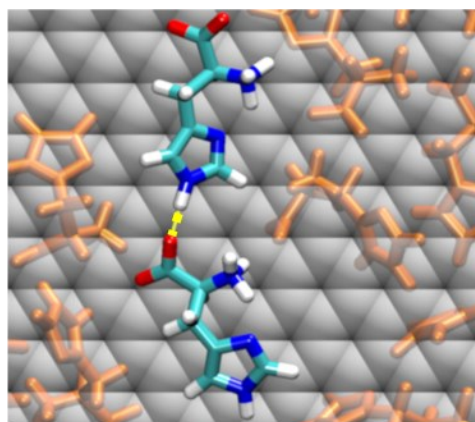


ND1-HE2-NE2 (Ring-Ring)

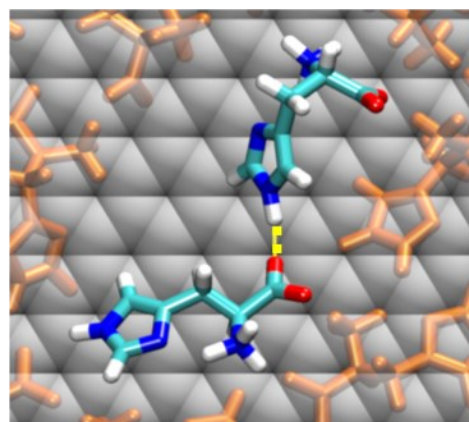


OT1-H-OT2 (C term-C term)

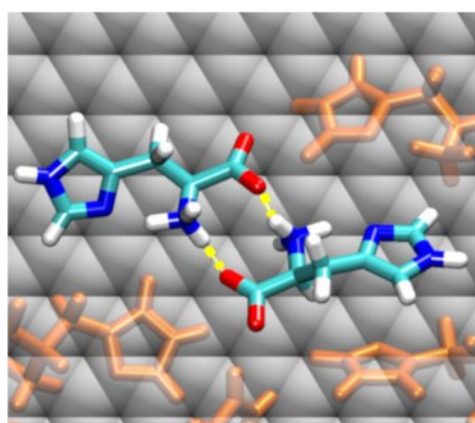
Figure S16 Snapshots of representative hydrogen bonding configurations formed within adsorbed neutral histidine adlayers on the graphene surface. Hydrogen bonds shown in yellow colour. Surrounding histidines in the adlayer are shown in translucent orange.



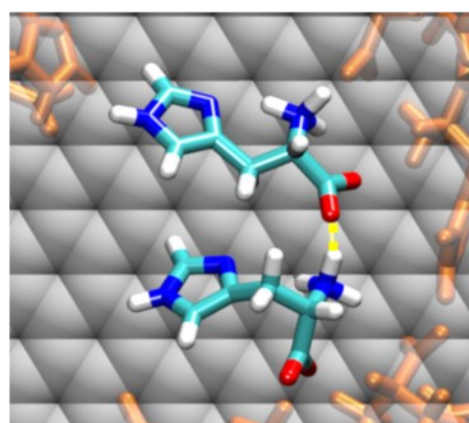
OT1-HE2-NE2 (C term-Ring)



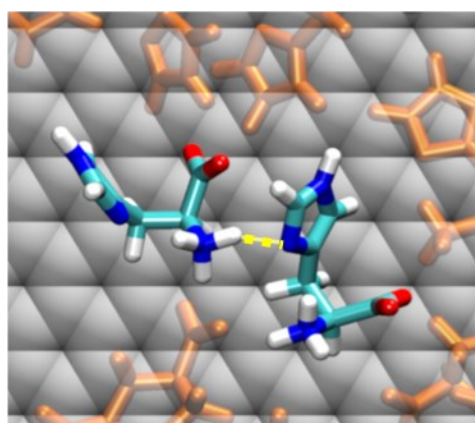
OT2-HE2-NE2 (C term-Ring)



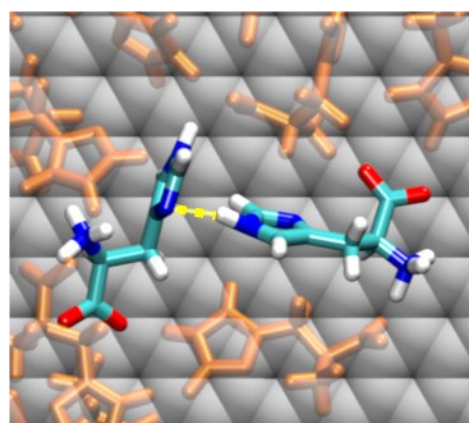
OT1-HT-N (C term-N term)



OT2-HT-N (C term-N term)



ND1-HT-N (Ring-N term)



ND1-HE2-NE2 (Ring-Ring)

Figure S17 Snapshots of representative hydrogen bonding configurations formed within adsorbed zwitterion histidine adlayers on the graphene surface. Hydrogen bonds shown in yellow colour. Surrounding histidines in the adlayer are shown in translucent orange.

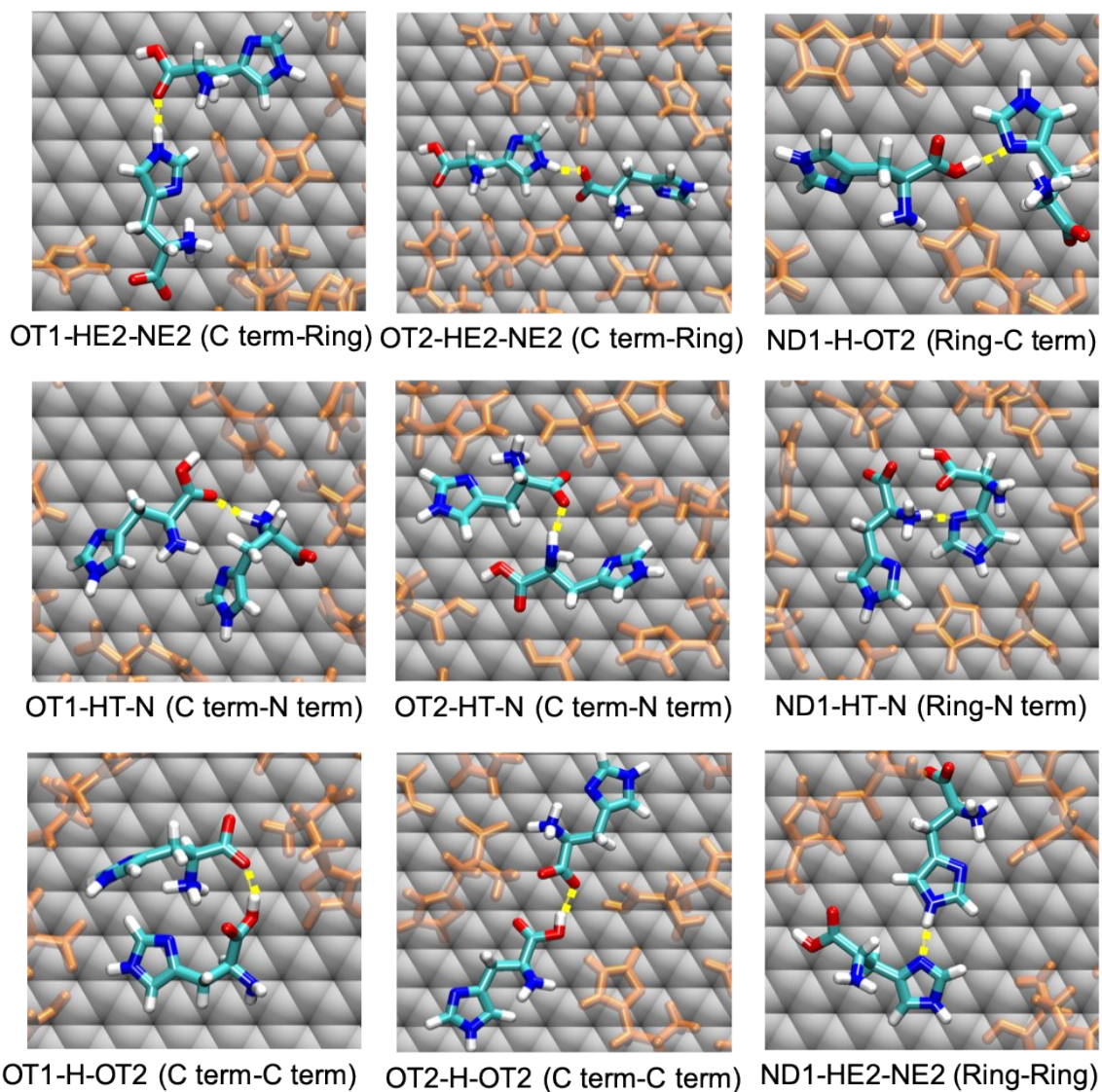
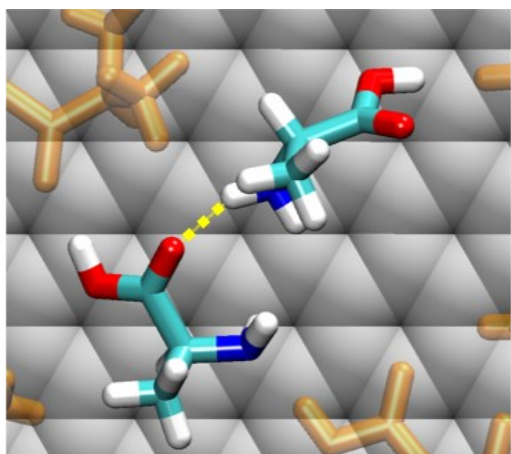
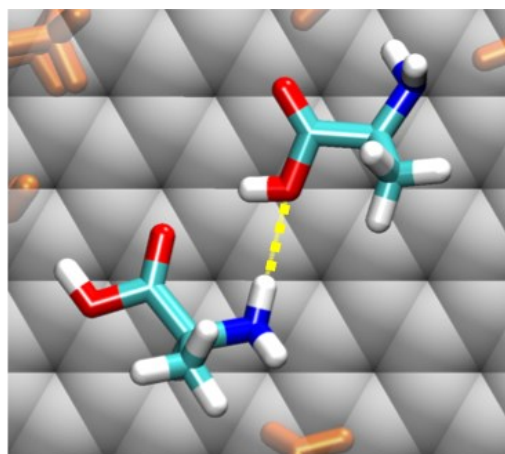


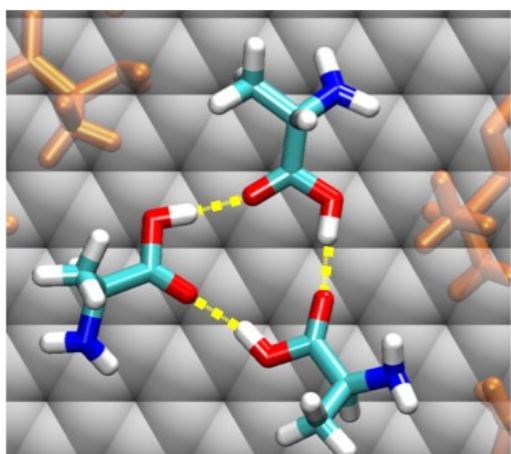
Figure S18 Snapshots of representative hydrogen bonding configurations formed within adsorbed mixed histidine adlayers on the graphene surface. Hydrogen bonds shown in yellow colour. Surrounding histidines in the adlayer are shown in translucent orange.



OT1-HT-N (C term-N term)

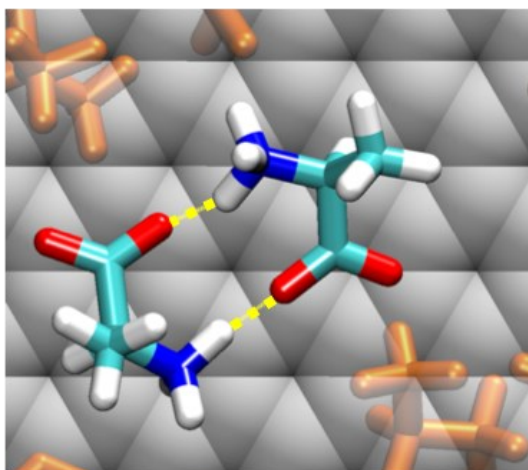


OT2-HT-N (C term-N term)

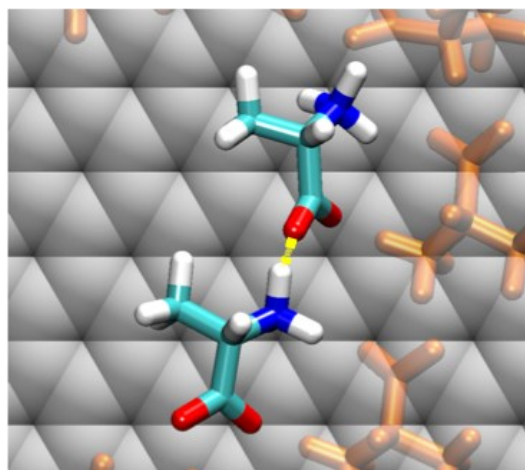


OT1-H-OT2 (C term-C term)

Figure S19 Snapshots of representative hydrogen bonding configurations formed within adsorbed neutral alanine adlayers on the graphene surface. Hydrogen bonds shown in yellow colour. Surrounding alanines in the adlayer are shown in translucent orange.

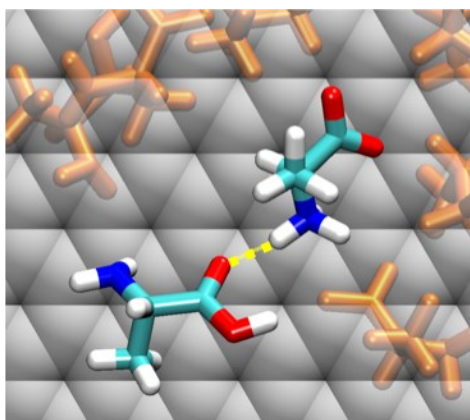


OT1-HT-N (C term-N term)

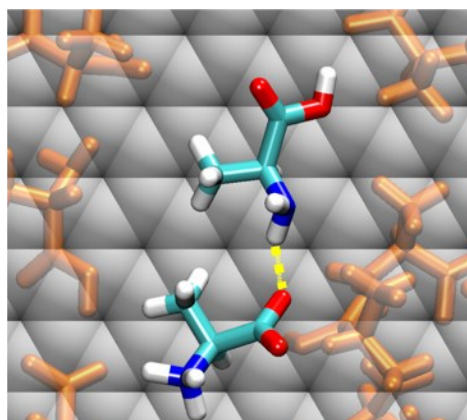


OT2-HT-N (C term-N term)

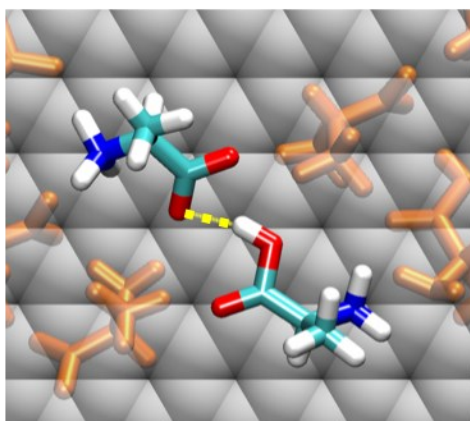
Figure S20 Snapshots of representative hydrogen bonding configurations formed within adsorbed zwitterion alanine adlayers on the graphene surface. Hydrogen bonds shown in yellow colour. Surrounding alanines in the adlayer are shown in translucent orange.



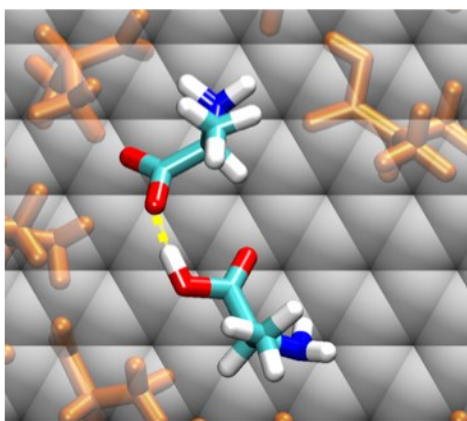
OT1-HT-N (C term-N term)



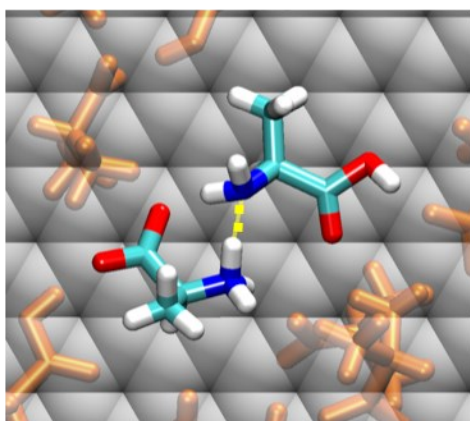
OT2-HT-N (C term-N term)



OT1-H-OT2 (C term-C term)



OT2-H-OT2 (C term-C term)



N-HT-N (N term-N term)

Figure S21 Snapshots of representative hydrogen bonding configurations formed within adsorbed mixed alanine adlayers on the graphene surface. Hydrogen bonds shown in yellow colour. Surrounding alanines in the adlayer are shown in translucent orange.

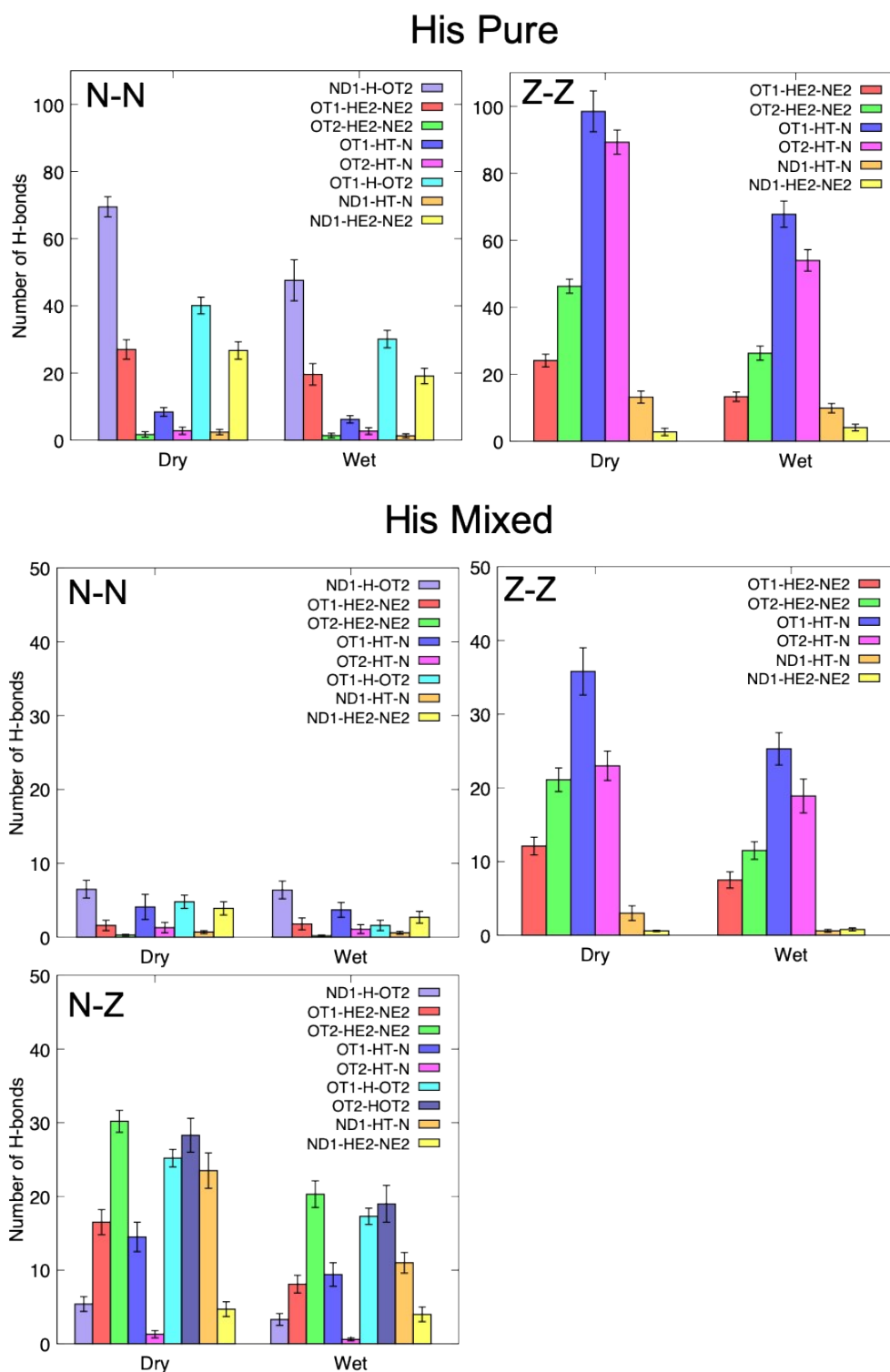


Figure S22 Simulated annealing molecular dynamics simulation data showing the average number of inter-amino acid hydrogen bonds formed within the first layer of the adsorbed pure (a) and mixed (b and c) histidine adlayers on the graphene surface. N-N, Z-Z and N-Z represent neutral-neutral, zwitterion-zwitterion and neutral-zwitterion interactions respectively.

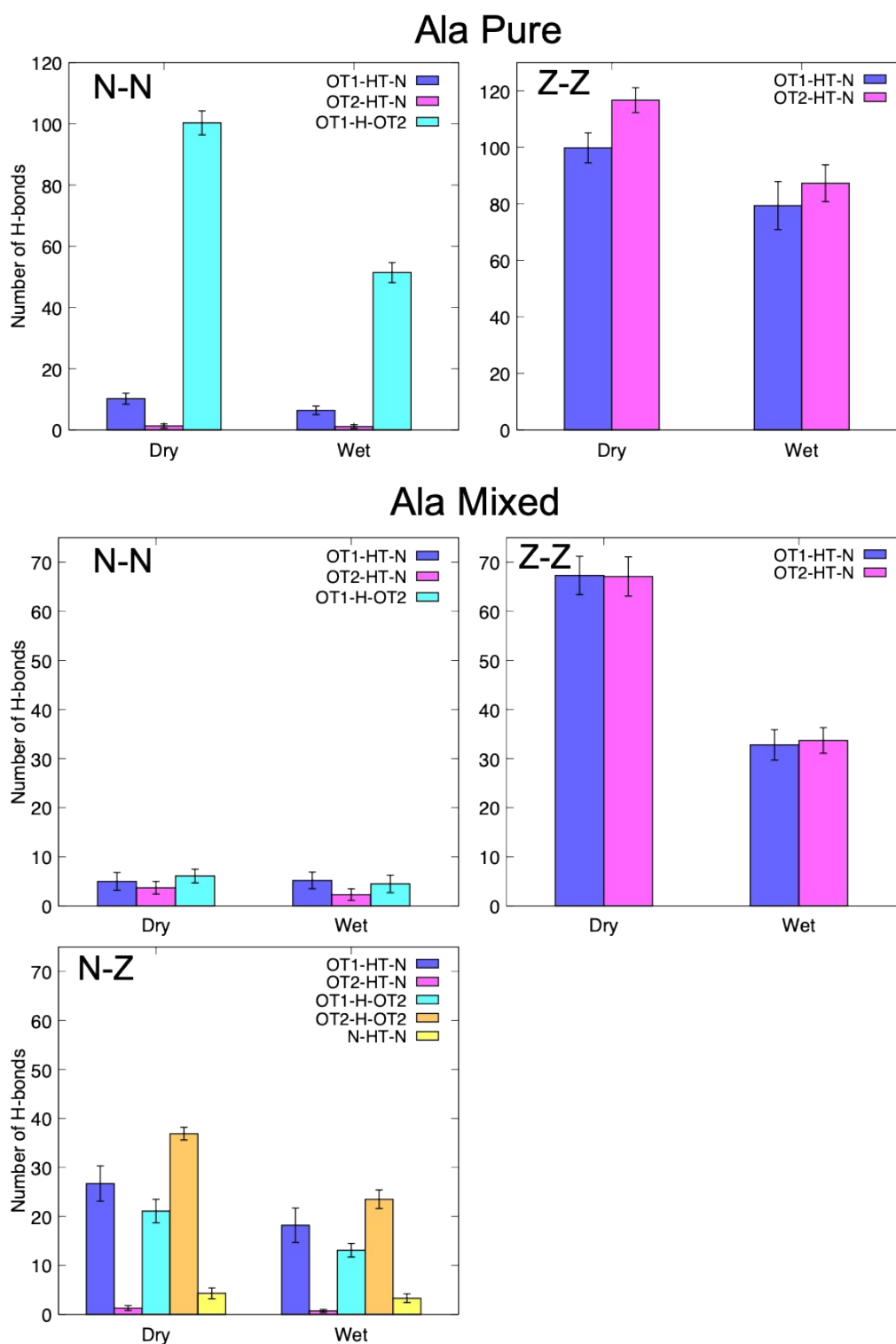
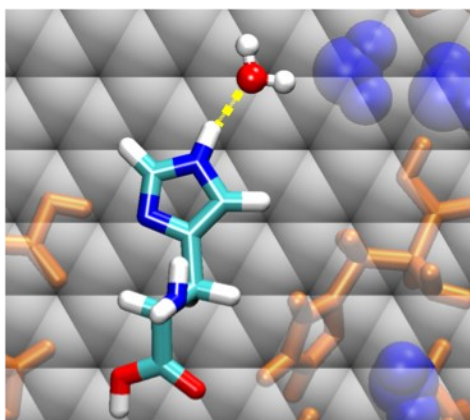
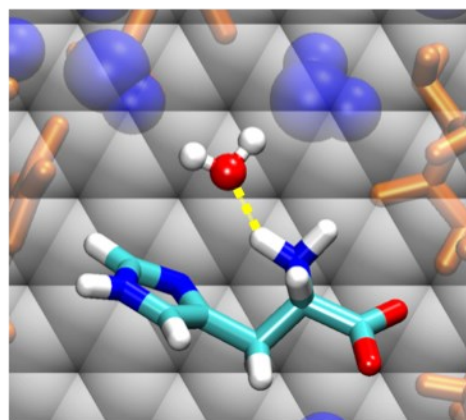


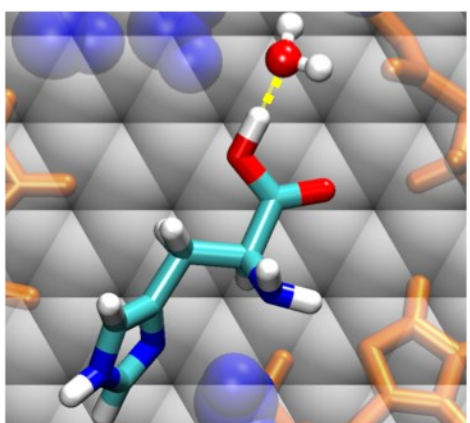
Figure S23 Simulated annealing molecular dynamics simulation data showing the average number of inter-amino acid hydrogen bonds formed within the first layer of the adsorbed pure (a) and mixed (b and c) alanine adlayers on the graphene surface. N-N, Z-Z and N-Z represent neutral-neutral, zwitterion-zwitterion and neutral-zwitterion interactions respectively.



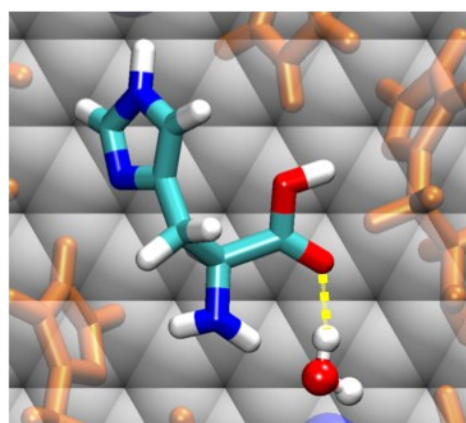
OW-HE2-NE2 (Water-Ring)



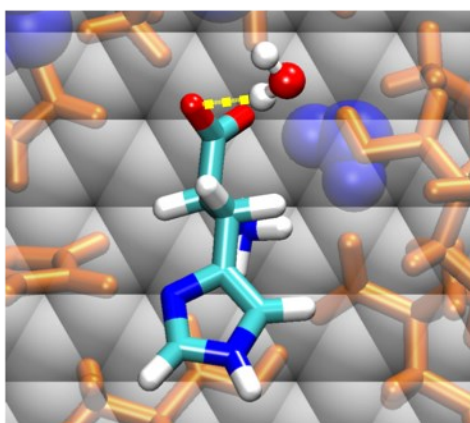
OW-HT-N (Water-N term)



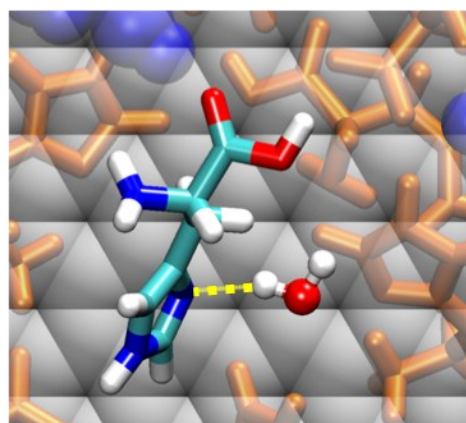
OW-H-OT2 (Water-C term)



OT1-HW-OW (C term-Water)

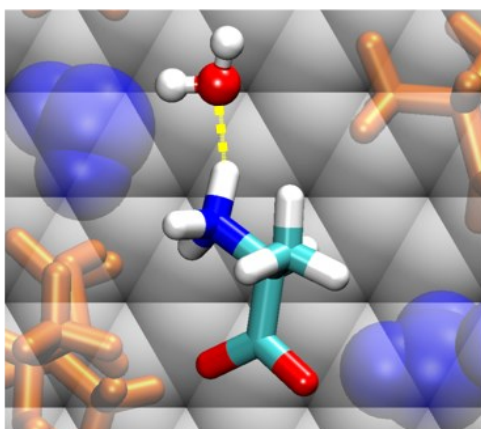


OT2-HW-OW (C term-Water)

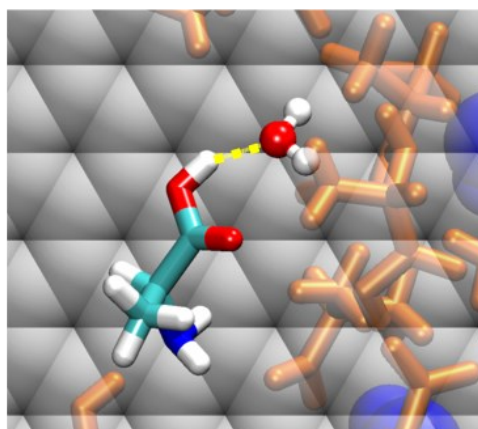


ND1-HW-OW (Ring-Water)

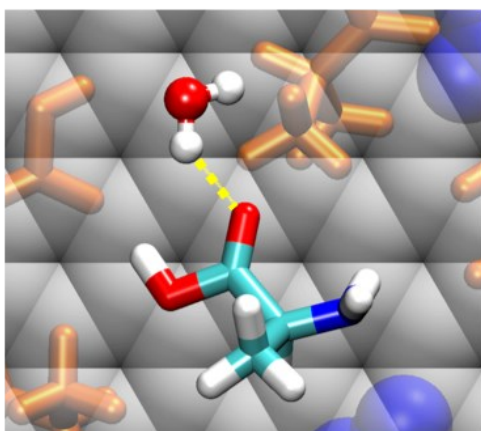
Figure S24 Snapshots of representative water-amino acids hydrogen bonding configurations within the adsorbed histidine adlayers at wet graphene interface. Hydrogen bonds are shown in yellow colour. Surrounding histidines in adlayer and water are shown in translucent orange and blue respectively.



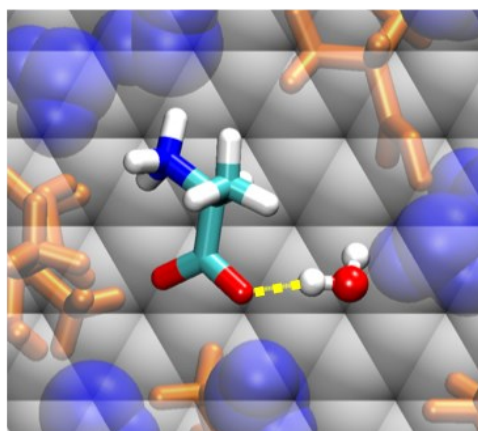
OW-HT-N (Water-N term)



OW-H-OT2 (Water-C term)



OT1-HW-OW (C term-Water)



OT2-HW-OW (C term-Water)

Figure S25 Snapshots of representative water-amino acids hydrogen bonding configurations within the adsorbed alanine adlayers at wet graphene interface. Hydrogen bonds are shown in yellow colour. Surrounding alanines in adlayer and water are shown in translucent orange and blue respectively.

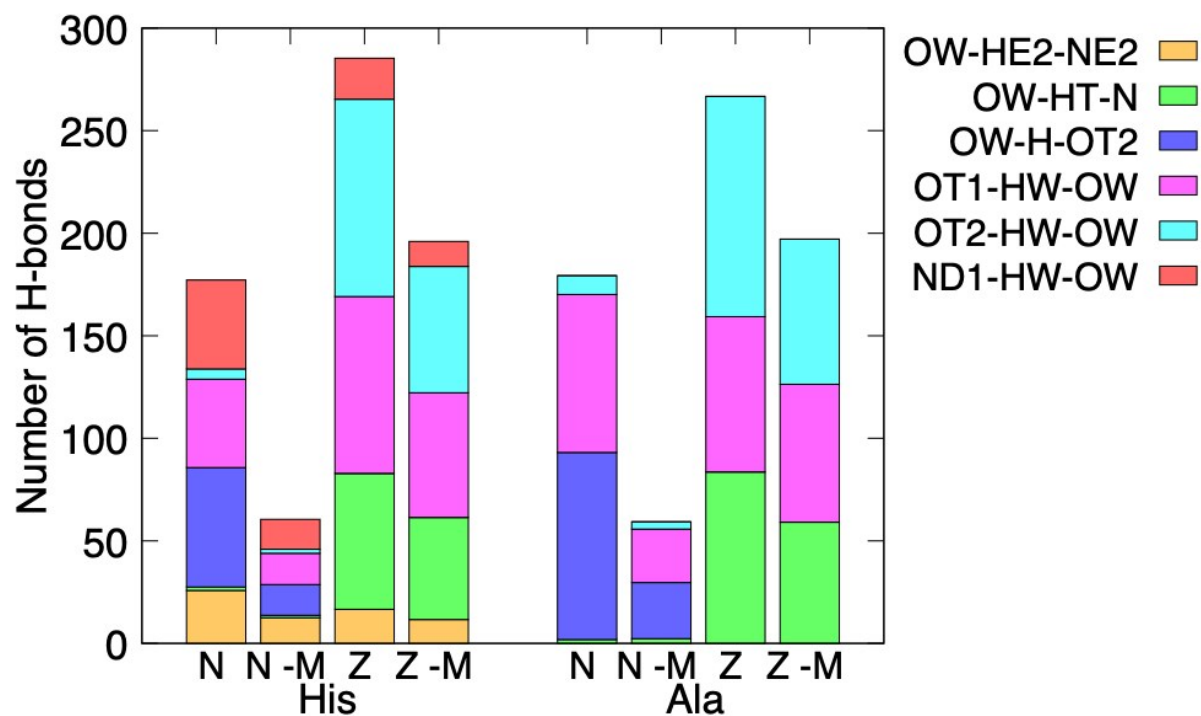


Figure S26 Simulated annealing molecular dynamics simulation data showing the total number of water-amino acids hydrogen bonds formed within histidine and alanine adlayers at the wet graphene interface. N and Z represent hydrogen bonding within pure neutral and zwitterion adlayers respectively. N -M and Z -M represent water-neutral and water-zwitterion hydrogen bonding within the mixed adlayers respectively.

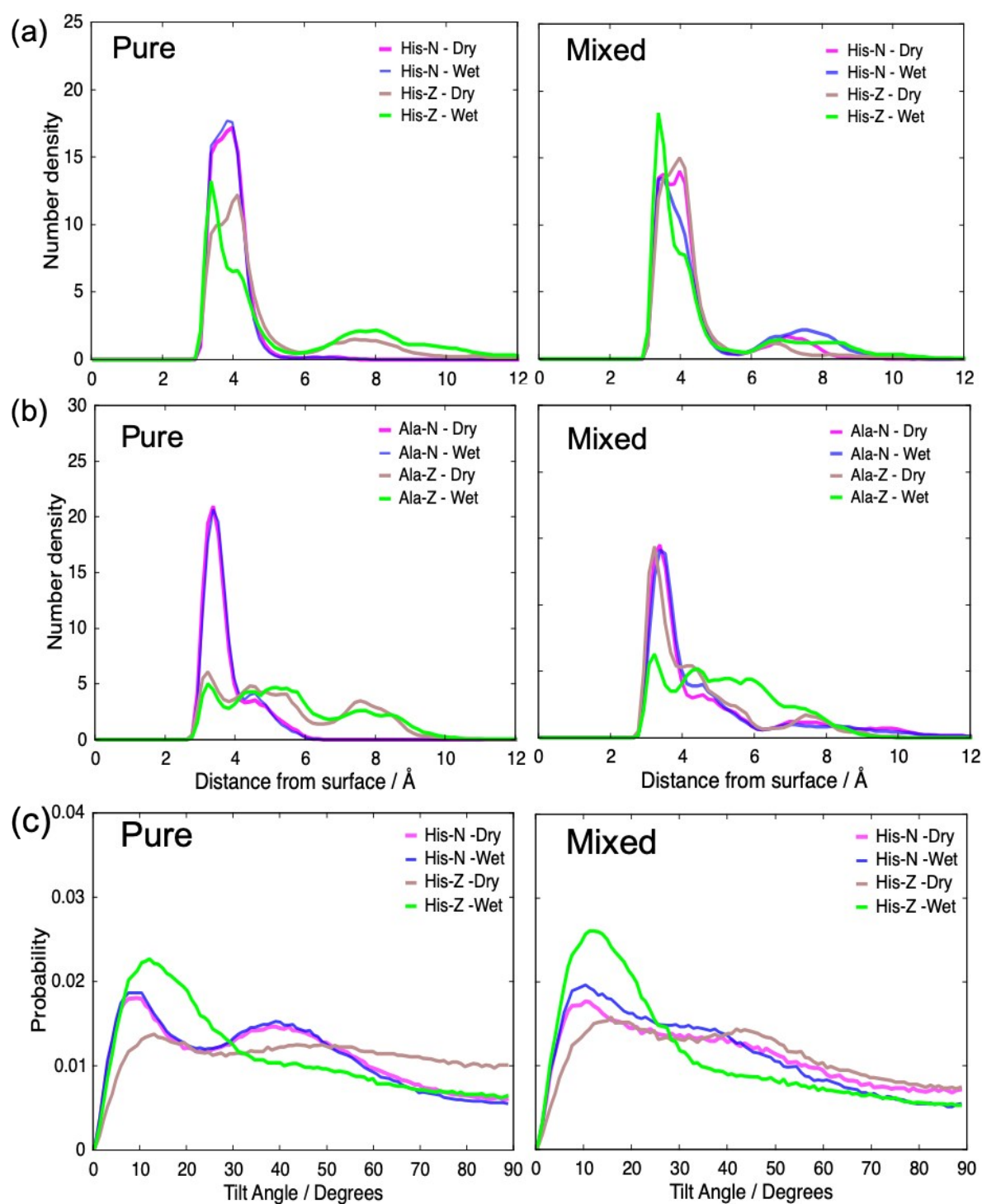


Figure S27 Simulated annealing molecular dynamics (SAMD) simulation data showing the vertical density profiles with respect to the distance between (a) the centre of histidine rings in the adlayers and graphene, and (b) the N term of alanine in the adlayers and graphene. (c) The probability distribution of the tilt angle between the histidine rings in the adlayers and the graphene surface, when the alpha-carbon (C_α) was within 6.5 Å of the graphene surface.

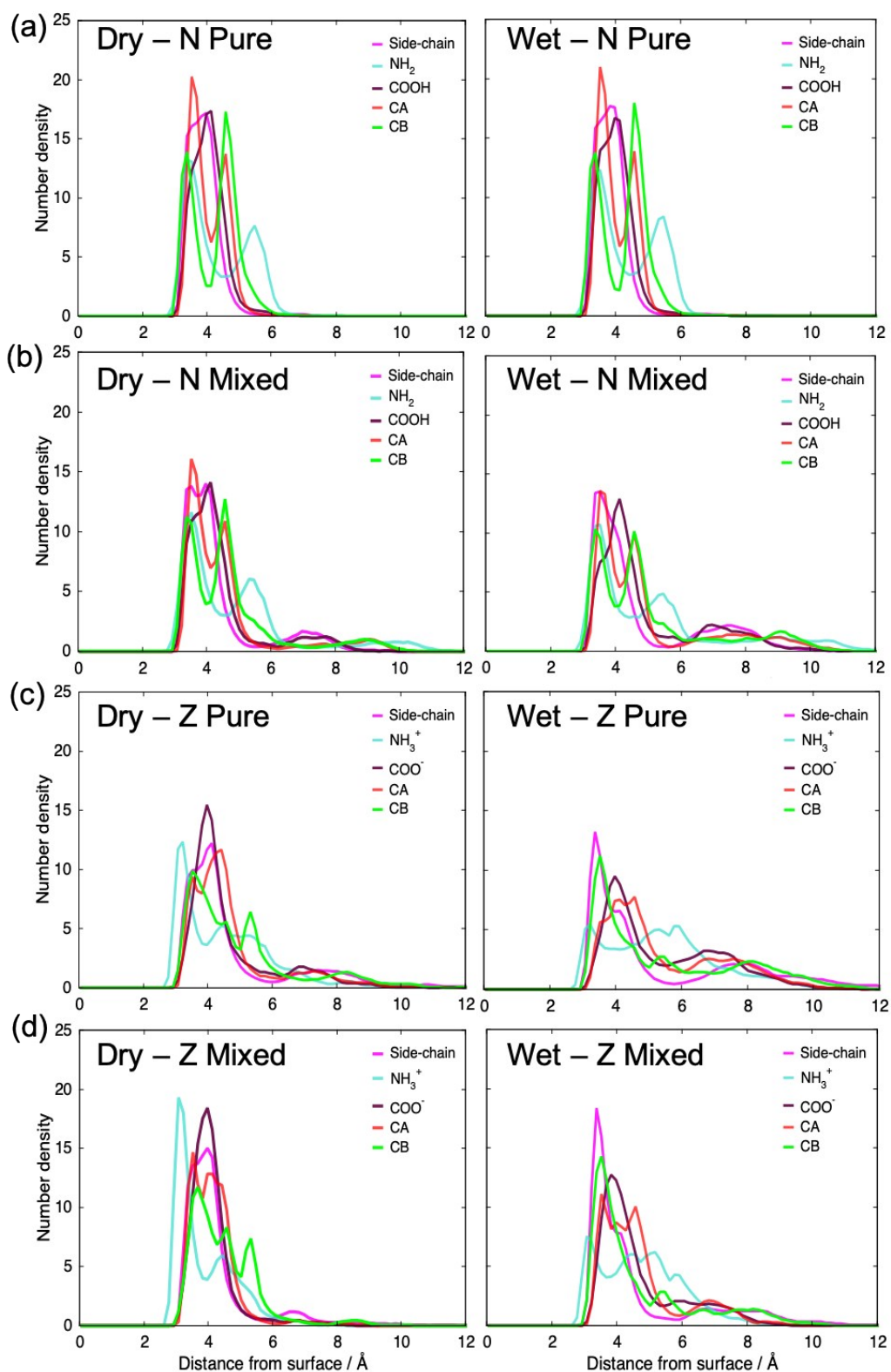


Figure S28 Simulated annealing molecular dynamics (SAMD) simulation data showing the vertical density profiles with respect to the distance between neutral (a and b) and zwitterion (c and d) histidine and graphene for the adsorbed pure adlayers (a and c) and mixed adlayers (b and d) on the graphene surface.

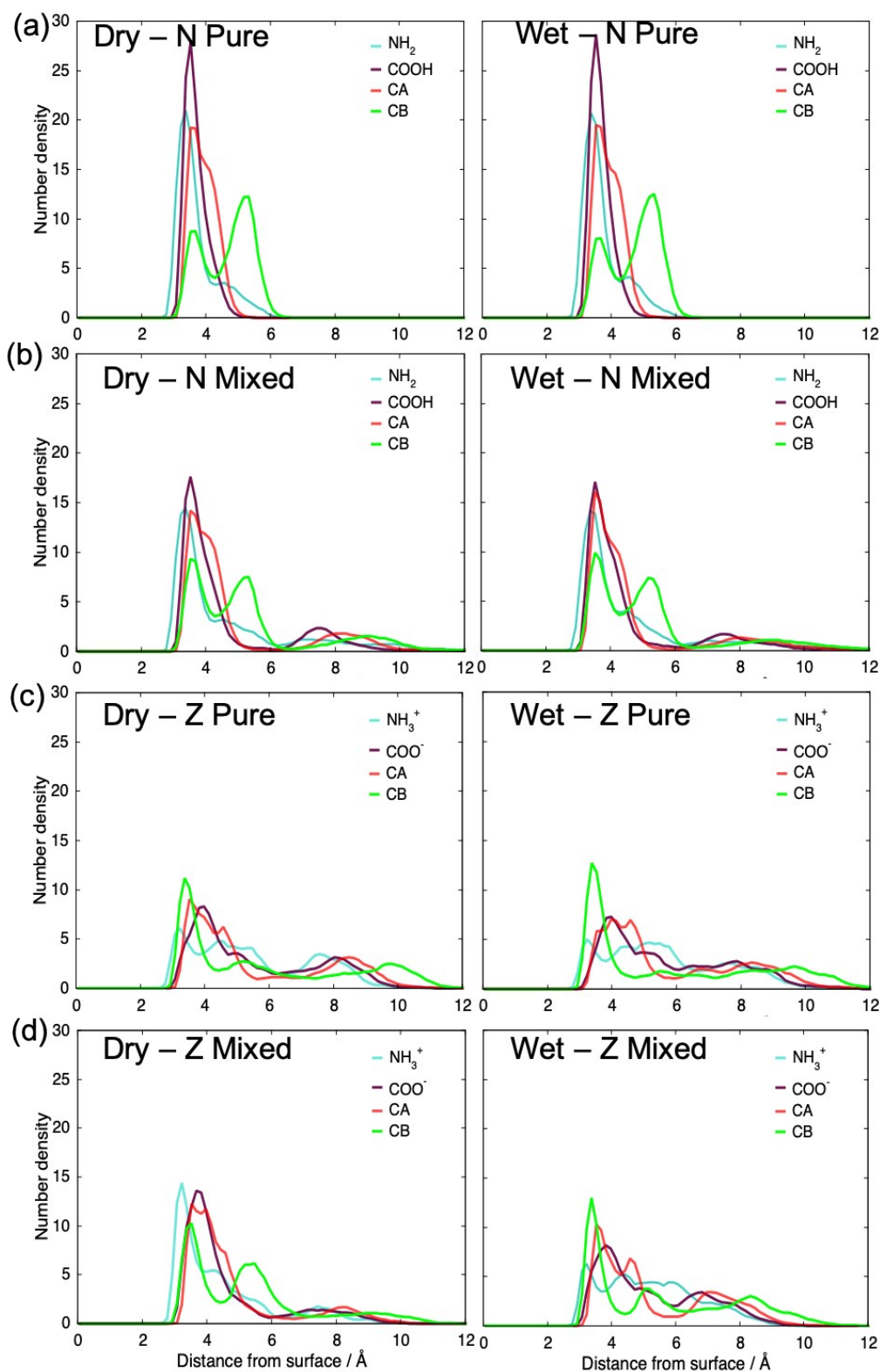


Figure S29 Simulated annealing molecular dynamics (SAMD) simulation data showing the vertical density profiles with respect to the distance between neutral (a and b) and zwitterion (c and d) alanine and graphene for the adsorbed pure adlayers (a and c) and mixed adlayers (b and d) on the graphene surface.

Table S3 Averaged structural properties of neutral amino acids calculated from simulated annealing molecular dynamics (SAMD). Interfacial separation distances, d_{sep} (Å), between neutral histidines and alanines in the adsorbed adlayer and graphene, and tilt angle between aromatic ring and graphene surface. Where applicable, two numbers indicate the position of pronounced peak one and two respectively.

Interactions	His		Ala	
	Dry	Wet	Dry	Wet
C _{graphene} -NH ₂	3.4/5.5	3.4/5.5	3.3	3.3
C _{graphene} -COOH	3.1	4.1	3.5	3.5
C _{graphene} -CA	3.5/4.6	3.5/4.6	3.5	3.5
C _{graphene} -CB	3.5/4.6	3.5/4.6	3.5/5.3	3.5/5.3
C _{graphene} -Side-chain	3.7	3.7		
Tilt Angle (°)	9/40	9/40		

Table S4 Averaged structural properties of zwitterion amino acids calculated from simulated annealing molecular dynamics (SAMD). Interfacial separation distances, d_{sep} (Å), between zwitterionic histidines and alanines in the adsorbed adlayer and graphene, and tilt angle between aromatic ring and graphene surface. Where applicable, two numbers indicate the position of pronounced peak one and two respectively.

Interactions	His		Ala	
	Dry	Wet	Dry	Wet
C _{graphene} -NH ₃ ⁺	3.2/5.8	3.2/5.8	3.3	3.3
C _{graphene} -COO ⁻	4.0	4.0	4.0	4.0
C _{graphene} -CA	4.4	4.4	3.7	3.7
C _{graphene} -CB	3.5/5.3	3.5	3.5/5.3	3.5/5.3
C _{graphene} -Side-chain	3.7	3.5		
Tilt Angle(°)	13	13		

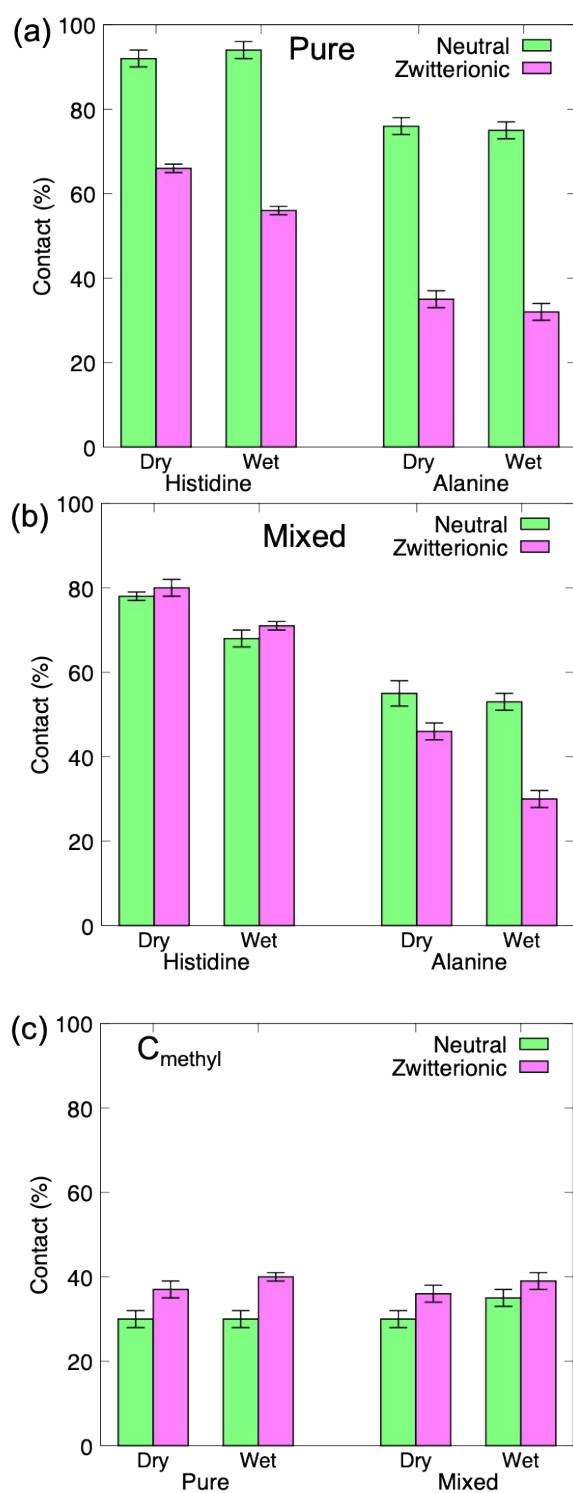


Figure S30 Percentage contact of the total number of neutral and zwitterion molecules in the adsorbed (a) pure (200) and (b) mixed (100) adlayers at graphene interfaces. (c) Percentage contact for alanine's methyl side-chain with the graphene surface.

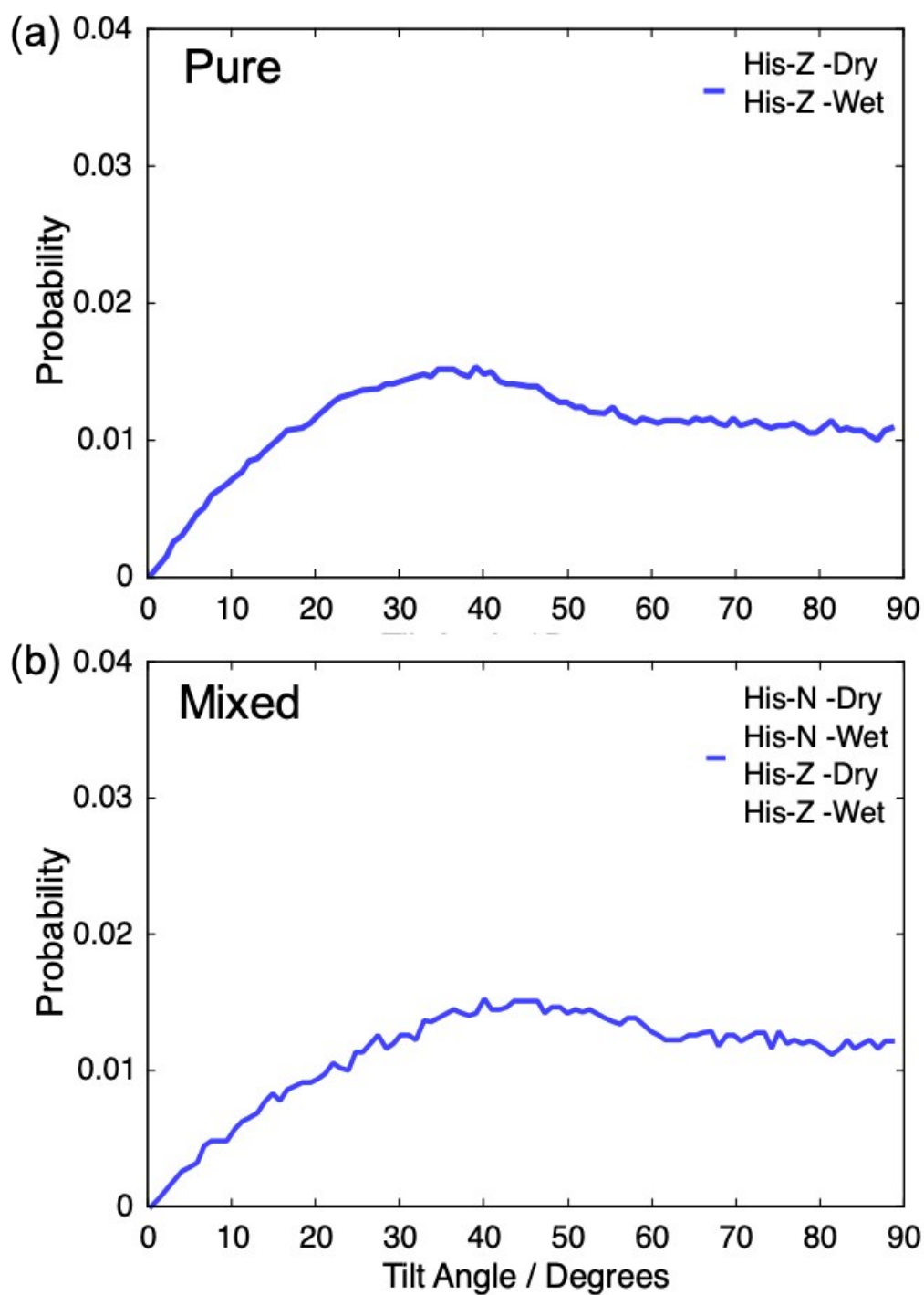


Figure S31 The probability distributions of the tilt angle between the histidine rings in the adlayers and the graphene surface, when the alpha-carbon (C_α) was located further than 6.5 Å but within 13 Å (C_α -graphene) of the graphene surface.

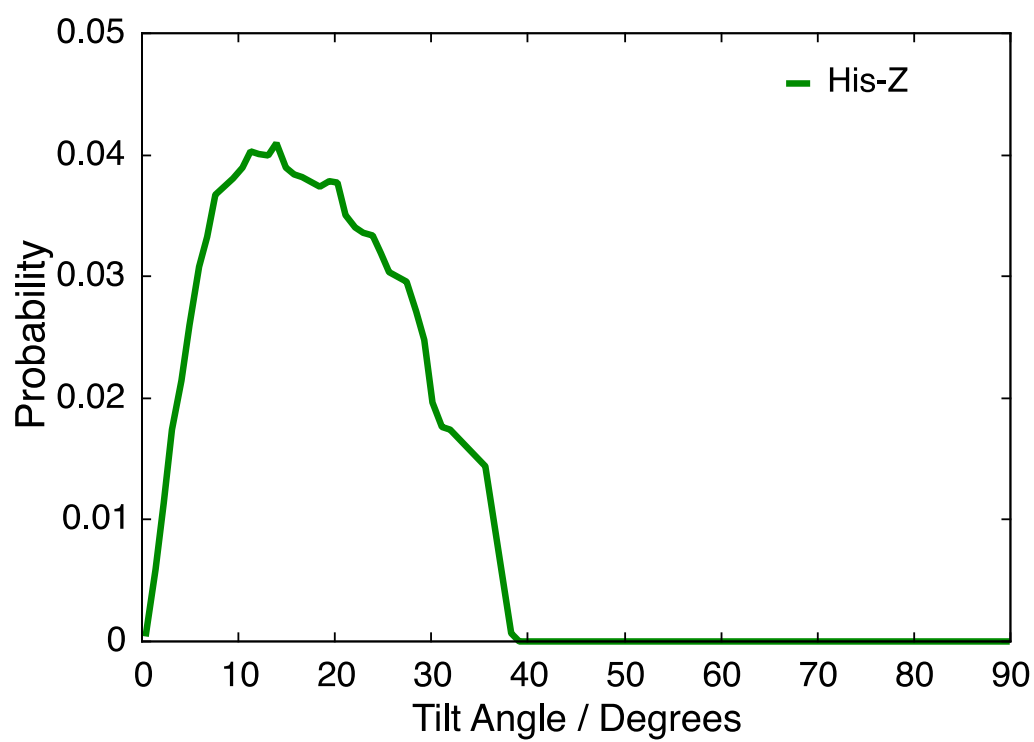


Figure S32 The probability distributions of the tilt angle between histidine rings in the staggered dimer row motif and the graphene surface.

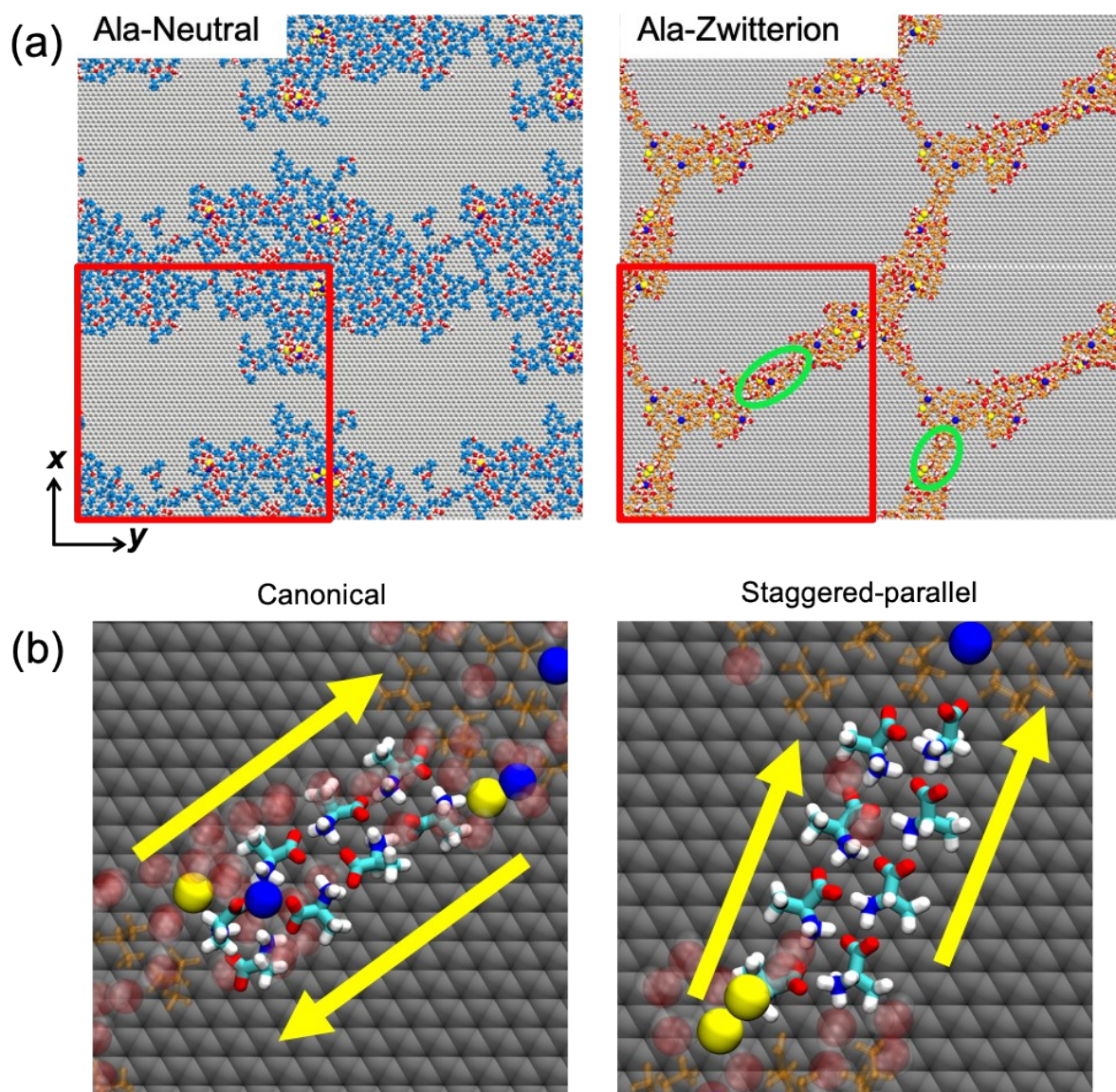


Figure S33 (a) Snapshots of representative morphologies of the wet neutral and zwitterion alanine adlayers with ion contaminants on graphene surface (2×2 supercell). Graphene sheet is shown in grey, neutral and zwitterion amino acids are shown in blue and orange respectively. Yellow and dark blue represent chlorine and sodium ions respectively. Red squares represent the simulation periodic boundaries. Green circles highlight incipient spontaneously emergent ordered motifs. (b) Snapshots of representative emergent ordered motifs within zwitterionic alanine adlayers with ion contaminants on wet graphene surface. Surrounding amino acids in the layer are shown in translucent orange. Yellow arrows indicate directions of the N-termini to C-termini along the row.